Journal of Medicinal Chemistry

Article

Lathyrol Diterpenes as Modulators of P-Glycoprotein Dependent Multidrug Resistance: Structure-Activity Relationship Studies on Euphorbia factor L3 Derivatives

Wei Jiao, Zhongmin Wan, Shuang Chen, Runhua Lu, Xiaozhen Chen, Dongmei Fang, Jiufeng Wang, Shengcai Pu, Xin Huang, Haixiang Gao, and Huawu Shao

J. Med. Chem., **Just Accepted Manuscript** • DOI: 10.1021/acs.jmedchem.5b00058 • Publication Date (Web): 09 Apr 2015

Journal of Medicinal Chemistry is published by the American Chemical Society. 1155 Sixteenth Street N.W., Washington, DC 20036

Lathyrol Diterpenes as Modulators of P-Glycoprotein Dependent Multidrug Resistance: Structure–Activity Relationship Studies on *Euphorbia* factor L_3 Derivatives

Wei Jiao,[*,1] Zhongmin Wan,[1] Shuang Chen,[1] Runhua Lu,[2] Xiaozhen Chen,[1] Dongmei Fang,[1] Jiufeng Wang,[1] Shengcai Pu,[1] Xin Huang,[1] Haixiang Gao,[2] Huawu Shao[*,1]

[1] *Chengdu Institute of Biology, Chinese Academy of Sciences, Chengdu 610041, China*

[2] *Department of Applied Chemistry, China Agricultural University, Beijing 100194, China*

Keywords: Lathyrol diterpene; Structure–activity relationship; *Euphorbia* factor L_3, Multidrug resistance; P-glycoprotein; *Euphorbia lathyris*

ABSTRACT:

Five series of 37 new acylate and epoxide derivatives (**3**-**39**) of *Euphorbia* factor L_3, a lathyrol diterpene isolated from *Euphorbia lathyris*, were designed by modifying the hydroxyl moiety of C-3, C-5 or C-15. Chemoreversal effects of the acylates on multidrug resistance (MDR) were evaluated in breast cancer multidrug-resistant MCF-7/ADR cells that overexpress P-glycoprotein (P-gp). Eight derivatives exhibited greater chemoreversal ability than verapamil (VRP) against adriamycin (ADR) resistance. Compounds **19** and **25** exhibited 4.8 and 4.0 times, respectively, more effective reversal ability than VRP

against ADR resistance. To determine the key characteristics of *Euphorbia* factor L_3 derivatives that contribute to MDR reversal, we conducted a structure–activity relationship study of these compounds. The simulation studies indicated different possible mechanisms and revealed the important influence of hydrophobic interactions and hydrogen bonds in the flexible cavity of P-gp.

INTRODUCTION

Recent estimates from the International Agency for Research on Cancer indicate a sharp increase in breast cancer incidence, with 14.1 million new cancer cases in 2012. Breast cancer incidence has increased by more than 20%, whereas mortality has increased by 14%, to estimates in 2008.[1] In cancer treatment, multidrug resistance (MDR) has been recognized as a major cause for the failure of chemotherapy. Additionally, MDR is an extensive problem implicated in numerous diseases, such as HIV infection and parasitic diseases.[2] Anthracyclines (*e.g.*, adriamycin (ADR), daunomycin, and epirubicin) are the most common oncology drugs used in combination therapy for breast cancers.[3] However, the response rates remain suboptimal, and curability is complicated by subclinical metastases and, eventually, distant metastases from MDR to breast cancer chemotherapy. In metastatic breast cancer and other metastatic cancers, drug resistance to chemotherapy is thought to result in treatment failure in greater than 90% of patients.[4]

The ABC (ATP binding cassette) transporter P-glycoprotein (P-gp, ABCB1) is one of the principal multidrug transporters in humans and has been intensively characterized in

recent decades.[5,6] In breast cancer, the levels of P-gp expression strongly correlated with drug resistance in the examined clinical specimens.[7] Intrinsic or acquired overexpression of P-gp dramatically reduces drug response, leading to poor clinical outcomes following chemotherapy. This protein is generally expressed at higher levels in epithelial cell surfaces throughout the body, such as in the liver, pancreas, kidney, colon, and jejunum,[8] as well as in blood-tissue barriers such as blood-mammary tissue, blood-brain, blood-testis, and blood-nerve barriers.[9-11] In addition to MDR in chemotherapy, P-gp is also closely associated with oral drug bioavailability, drug excretion, and brain permeation.[12] P-gp acts as an ATP-dependent drug efflux pump, analogous to a "hydrophobic vacuum cleaner" that removes numerous structurally dissimilar chemotherapeutic agents from the cell.[13] Recently, the inward-facing conformation of murine P-gp, which shares 87% sequence identity to human P-gp, has been refined to 3.8 Å resolution, which represents the highest resolution structure of a mammalian multidrug transporter to date.[14] The flexible internal cavity formed by two bundles of six TM (transmembrane) helices encloses a large volume of ~6000 Å within the lipid bilayer to which hydrophobic drugs can bind in various orientations and at different locations. As predicted from previous photoaffinity labeling studies[15,16] and cross-linking analyses,[17] the crystal structure exhibits a uniform drug-binding domain, and this large and flexible binding pocket hinders the development of new modulators of P-gp.

In the past decade, P-gp has been considered the most important MDR-modulating drug

target, and numerous reversal agents have been developed. Currently, a reversal agent is clinically unavailable. Modulators of P-gp generally do not directly kill MDR cells; rather, when combined with a cytotoxic agent, these agents restore chemotherapeutic efficacy.[6] However, most MDR modulators suffer clinically due to intrinsic toxicity, low affinity or undesired pharmacokinetic properties. In this regard, recent studies suggest natural products as potential MDR modulators due to their various structure types. As a promising example, macrocyclic diterpenes derived from *Euphorbia* have attracted considerable interest,[18,19] with a focus on two types of diterpenes: jatrophane[20-25] and lathyrane.[25-28] Polycyclicity and polyestericity are two significant characteristics in these two skeleton types. These diterpenes are substituted with a variety of acyl groups and possess 5/12- or 5/11/3-membered ring systems. For lathyrane diterpenes, the effect of the acyl side chains is thought to be a critical factor in MDR reversal.[22,24,28] Moreover, the fused epoxy ring within the skeleton variation also appears to play an essential role.[25,26] However, synthetic methods of selective acylation and intramolecular epoxidation have not been completed to enrich the limited variation of lathyrane diterpenes. In our previous studies, five different structure types of lathyrane diterpenes as potential P-gp modulators (lathyrol, jokinol, isolathyrol, epoxylathyrol and 7-hydroxylathyrol) were investigated.[29] All compounds exhibited reversal effects in MCF-7/ADR breast cancer cell lines *in vitro*. *Euphorbia* factor L_3, which is a lathyrol diterpene in the lathyrane family, exhibited substantial reversal activity in our previous studies. This diterpene is a principal

secondary metabolite from the seeds of *Euphorbia lathyris*, which is a common traditional Chinese herb whose seed oil contains 3-5% lathyrane diterpene esters.[30] Compared to other lathyrane types, lathyrol diterpenes possess an identical skeleton of a 5/11/3-membered ring system and three ester substituents characterized by a 6,17-double bond outside of the macrocycle. In addition to *Euphorbia* factors L_3 and L_8, only six lathyrol diterpenes have been identified to date, and none have been screened for MDR reversal activity.[31-35] Therefore, we conducted a structure–activity relationship (SAR) investigation of *Euphorbia* factor L_3 derivatives.

Herein, beginning from *Euphorbia* factor L_3, five series (I-V) of new acylates and epoxides were designed with modifications at the hydroxyl of C-3, C-5 or C-15. The absolute configuration and X-ray structures of representatives from each series were determined for definitive structural confirmation. These derivatives were evaluated *in vitro* using a chemoreversal assay and the rhodamine 123 (Rh123) accumulation assay in MCF-7/ADR cells, which are breast cancer multidrug resistant cells that overexpress P-gp. The interaction patterns of **14**, **19** and **25** with a homology model of human P-gp in a lipid bilayer membrane environment were investigated using molecular modeling approaches.

RESULTS AND DISCUSSION

Chemistry. The known macrocyclic diterpene, *Euphorbia* factor L_3 (**1**), was purified using a chromatographic method from the ethanol/acetone extract of *E. lathyris* seeds.

We selected *Euphorbia* factor L_3 as the initial structure for the design of various esters, **3–39**, to assess substituents at positions C-3, C-5 and C-15 of the epoxide. The ester groups (R in Scheme 1) were selected considering the size, hydrophobicity, and aromaticity. The diverse set of substituents included aliphatic acyclic and aromatic groups.

Alkaline hydrolysis of *Euphorbia* factor L_3 afforded lathyrol **2** with three free hydroxyl groups. Esterifications of **2** were performed by treatment with the related acid (RCO_2H), *N*-(3-dimethylaminopropyl)-*N*′-ethylcarbodiimide hydrochloride (EDCI), and 4-dimethylaminopyridine (DMAP) to produce **3–9** and **11–14**. The esters **10**, **15** and **19** were achieved by treatment with benzoic anhydride, acetic anhydride or benzoyl chloride together with Et_3N and DMAP, depending on the different reactivity. It is difficult to distinguish the reactivity between OH-3 and OH-5; thus, several synthetic strategies were employed. The synthesis of **16**-**18** was conducted beginning from **2**, which was treated with a related acid anhydride and $BF_3{\cdot}Et_2O$. The acylation of **2** with RCO_2H, EDCI and DMAP yielded **20**-**22**. The derivatization of the related monosubstituted ester at C-3 using acid anhydride or ROCl and $BF_3{\cdot}Et_2O$ afforded **23**-**27**. $BF_3{\cdot}Et_2O$ was successfully used to address different substituents of C-3 and C-5 in *Euphorbia* diterpenes for the first time. Groups III (**28**) and IV (**29**-**31**) were prepared by acid-catalyzed intramolecular oxa-Michael addition with the Lewis acid TMSOTf. Group V was synthesized by epoxidation with AcCl and DMAP, affording **32**-**37** and **39**. The one-pot synthetic route

used to prepare **38** involved treatment with cinnamoyl chloride and $BF_3 \cdot Et_2O$ at 0 °C. Two new synthetic paths of intramolecular epoxidation on lathyrol diterpenes were discovered through the preparation of Group III, IV and V derivatives. Interestingly, selective intramolecular oxa-Michael addition under different conditions resulted in two C-13 epimers (Groups IV and V). These epoxides, which possess various ester groups, were further investigated, not only for the effect of the epoxy ring[25,26] but also for cytotoxic activity in a similar skeleton.[36] The X-ray structures of representative molecules are shown in Figure 1. The absolute configurations of these derivatives were determined according to the X-ray analysis of **17**.

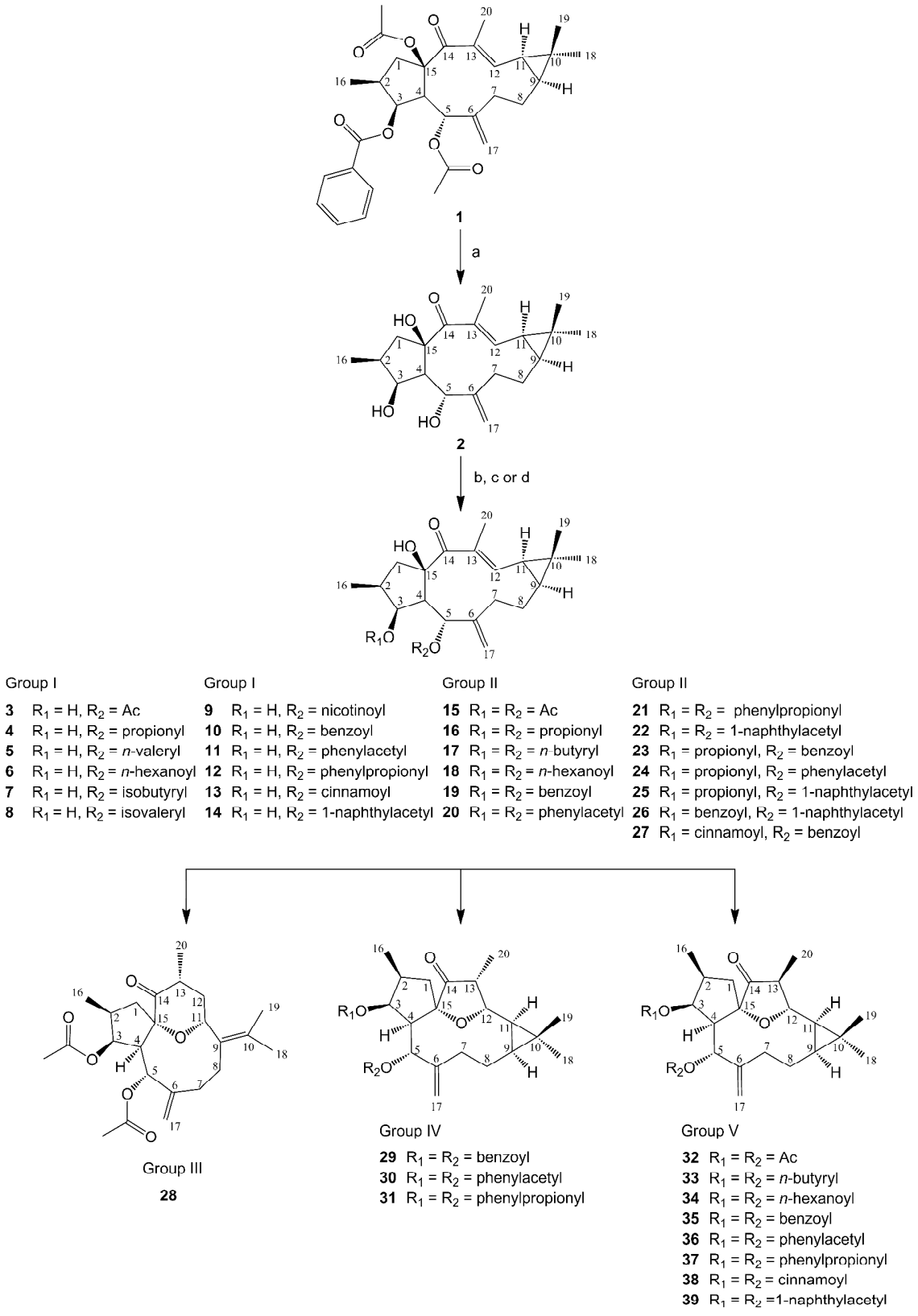

Scheme 1. Synthesis of *Euphorbia* factor L_3 derivatives[a]

[a]Reagents and conditions: (a) 5% KOH; (b) RCO_2H, EDCI, DMAP; (c) acid anhydride or ROCl, Et_3N, DMAP; (d) acid anhydride or ROCl, $BF_3 \cdot Et_2O$; (e) TMSOTf; (f) AcCl, DMAP; **38** was afford by treated with cinnamoyl chloride and $BF_3 \cdot Et_2O$ from **2**.

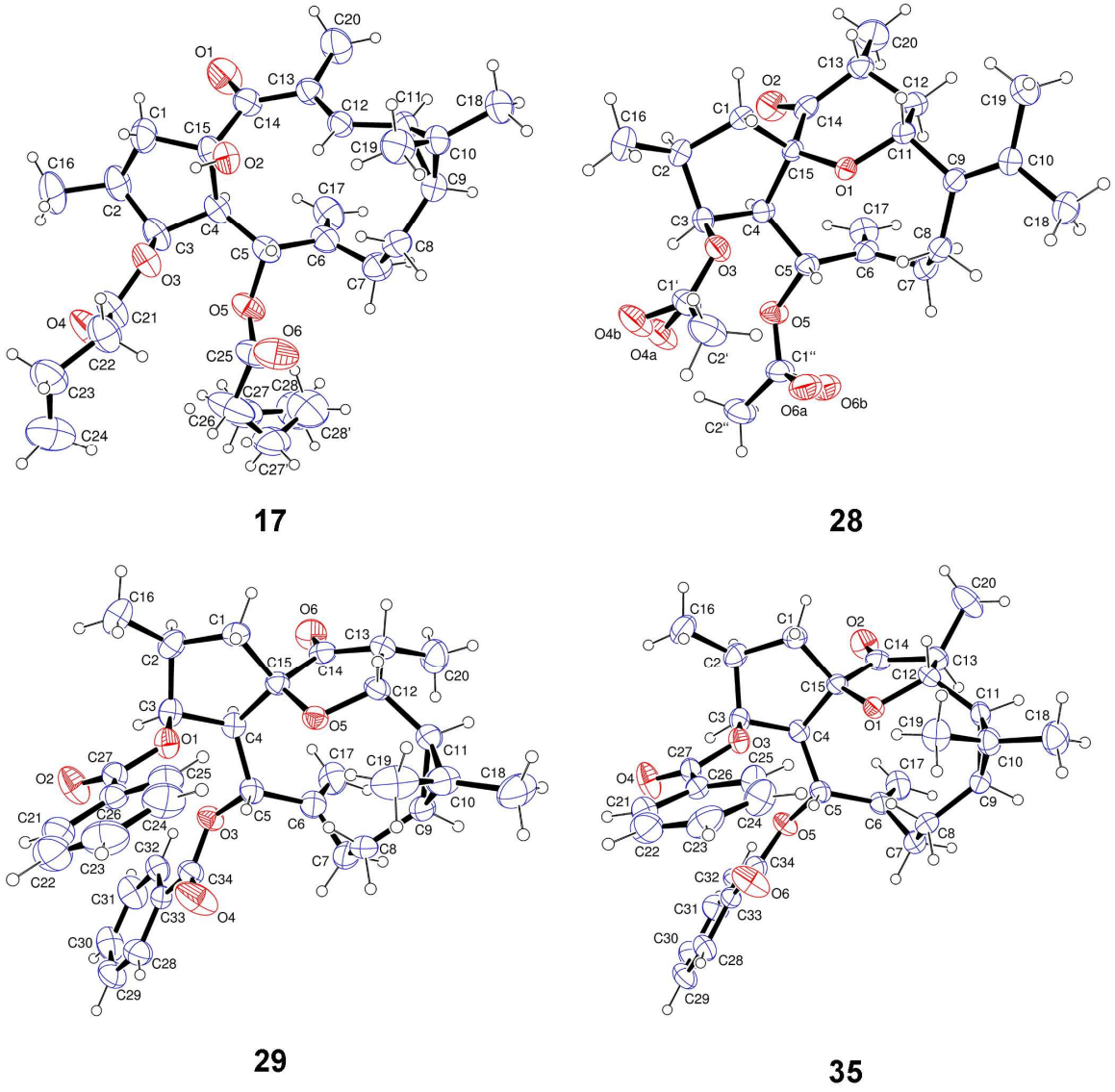

Figure 1. Views of the representative crystal structures: compound 17 (Group II), compound 28 (Group III), compound 29 (Group IV), compound 35 (Group V). Displacement ellipsoids are drawn at the 30% probability level. C27 and C28 of 17 are disordered. O4 and O6 of 28 are disordered.

Cytotoxicity Assay and Preliminary MDR Reversal Activity Screening. The cytotoxic

activity of *Euphorbia* factor L_3 derivatives (**2–39**) was evaluated in MCF-7 (human breast cancer) and MCF-7/ADR (an MDR subline overexpressing P-gp) cell lines using the SRB (sulforhodamine B) assay.[37] The IC_{50} values are presented in Table 1. All of the derivatives exhibited significantly greater cytotoxicity in MCF-7 cells than in MCF-7/ADR cells. Certain compounds (**18**, **21**, **22**, **26**, **29** and **32**-**39**) exhibited toxicity greater than 100 μM in MCF-7/ADR cells, which is beyond the scope of this investigation; therefore, only the trend in activity is outlined. In Group V, all of the *13S*-epoxylathyrol analogs (**32**-**39**) exhibited low toxicity (IC_{50} > 100 μM) in MCF-7/ADR cells. These results suggested that the parental cells were more sensitive to the test derivatives. For rapid evaluation of chemoreversal activity, MCF-7/ADR cells were cotreated with ADR and test compounds at 10 μM (Table 2). Nineteen derivatives were found to be superior to verapamil (VRP) in initial screens. From these results, the Group I (**4**, **6**, **7**, **10**-**14**), II (**19**, **20**, **22**-**27**) and V (**32**, **36**, **39**) derivatives were emphatically observed.

Table 1. Cytotoxicity Effects of 2-39 on MCF-7 Cells (PAR Cells) and MCF-7/ADR (MDR Cells)

compd	IC_{50} (μM)[a]	
	PAR cell	MDR cell
2	34.04±1.84	59.56±3.57
3	26.62±1.52	80.72±3.13
4	32.09±2.26	53.46±1.84
5	13.11±1.61	57.90±3.12
6	18.07±1.65	46.06±1.53
7	17.00±0.84	66.29±4.20

8	14.78±2.09	60.77±6.57
9	17.26±3.78	19.27±4.63
10	11.60±0.36	55.27±6.63
11	14.82±2.46	42.90±1.53
12	10.99±1.59	23.45±1.70
13	8.24±0.92	58.79±3.90
14	10.46±1.36	33.67±2.51
15	21.56±2.87	40.96±5.06
16	18.55±1.79	44.98±1.01
17	18.51±2.58	50.86±0.96
18	47.10±4.96	>100
19	13.17±0.59	63.77±2.77
20	8.93±1.69	36.26±2.56
21	28.69±4.01	>100
22	13.36±0.60	>100
23	8.47±1.00	63.27±5.05
24	9.57±1.54	76.03±1.58
25	9.73±1.35	75.67±1.71
26	4.16±0.93	>100
27	14.18±2.80	42.12±1.92
28	45.78±7.59	65.16±6.16
29	25.25±3.09	>100
30	28.50±1.41	54.96±5.48
31	14.15±1.49	40.08±4.64
32	12.67±1.44	>100
33	19.14±2.70	>100
34	48.15±4.60	>100
35	34.93±4.45	>100
36	28.47±6.08	>100
37	46.76±4.47	>100
38	64.22±4.33	>100
39	84.87±1.00	>100
Taxol	$4.42\times10^{-3}\pm9.72\times10^{-4}$	$4.36\times10^{-2}\pm4.46\times10^{-3}$

[a] Values of IC_{50} are the mean ± standard error (SD) of three independent experiments.

Chemoreversal Abilities of *Euphorbia* Factor L_3 Derivatives against ADR Resistance.

The reversal abilities of the *Euphorbia* factor L_3 derivatives (**2–39**) were evaluated using MCF-7/ADR cells with gradient concentrations of the chemotherapeutic drug ADR. The

EC_{50} value of ADR was calculated by cotreatment with the derivatives at 10 μM. The reversal fold was determined by dividing the EC_{50} of ADR alone by the EC_{50} of the combination treatment.

Table 2. Multidrug Resistance Reversal Effects of 2-39 on MCF-7/ADR

group	compd	relative enhancement intensity (%)[a]	EC_{50} (μM)[b]	fold[c]
I	2	7.3	11.63±1.89	3.0
	3	7.1	18.49±0.17	1.9
	4	11.3	15.18±1.33	2.3
	5	0.1	41.59±2.18	0.8
	6	9.1	11.45±1.03	3.0
	7	10.1	10.62±3.81	3.2
	8	4.7	8.41±1.08	4.1
	9	10.3	14.78±4.17	2.3
	10	7.5	22.39±3.19	1.5
	11	9.6	4.66±1.20	7.4
	12	11.6	9.89±0.21	3.5
	13	9.1	12.76±1.02	2.7
	14	15.5	2.15±0.36	16.0
II	15	4.7	8.37±1.71	4.1
	16	4.6	12.11±2.26	2.8
	17	4.0	14.49±1.20	2.4
	18	5.8	18.51±3.86	1.9
	19	23.9	1.00±0.12	34.4
	20	9.5	13.13±3.60	2.6
	21	6.0	27.04±3.40	1.3
	22	10.1	24.93±1.88	1.4
	23	12.1	4.22±1.12	8.2
	24	9.3	4.23±1.48	8.1
	25	14.4	1.21±0.65	28.6
	26	11.1	8.66±1.44	4.0
	27	12.1	3.53±0.76	9.8
III	28	2.4	18.61±0.97	1.9
IV	29	6.8	10.62±3.10	3.2
	30	4.0	21.03±1.57	1.6

	31	8.3	21.57±5.37	1.6
V	32	13.0	3.23±0.60	10.7
	33	7.7	11.52±2.10	3.0
	34	6.8	4.94±1.00	7.0
	35	4.3	20.49±3.88	1.7
	36	11.6	16.38±3.14	2.1
	37	6.9	29.17±2.43	1.2
	38	2.1	9.68±2.04	3.6
	39	10.4	25.10±0.94	1.4
	VRP	8.4	4.89±0.71	7.1

[a]Relative enhancement intensity of compounds were showed at concentration of 10 μM and calculated as equation in the section of MDR Reversal Activity. [b]EC_{50} (half maximal effective concentration) are the mean ± standard error (SD) of at least three independent experiments. [c]Reversal fold was calculated as equation in the section of MDR Reversal Activity.

As shown in Table 2, compounds **11**, **14**, **19**, **23**-**25**, **27** and **32** exhibited more potent chemoreversal ability than the positive control VRP. Compared to our previous studies, compounds **14**, **19** and **25** were more active than the parent structure, *Euphorbi*a factor L_3 (**1**). Notably, **19** was 4.8 times more effective than VRP in ADR reversal ability in MCF-7/ADR cells, and it was more effective than all *E. lathyris* diterpenes previously evaluated.[29] The MDR reversal activities of compounds **23**, **24**, **27** and **32** were slightly higher than that of VRP. Compounds **11** and **34** exhibited nearly an identical MDR reversal effect as VRP. Compounds that exhibited reversal fold values greater than 15.0 were classified as potential MDR modulators. The following SAR correlations were proposed based on the MDR reversal effect on ADR resistance.

In Group I, the monoacylated derivatives were synthesized to evaluate the substituent effect at C-5. In this group, the enhanced size of aliphatic (**3**-**8**) and aromatic (**9**-**14**)

substituents did not correspond to a proportional reversal activity. The presence of the normal alkyl chain exhibited a low effect, and acylation of the alkane isomers slightly improved the activity, as observed for **7** and **8**. Compared to the poor profiles of the aliphatic-substituent analogs, compounds **14** (R = 1-naphthylacetyl) and **11** (R = phenylacetyl) exhibited higher reversal fold (16.0 and 7.4, respectively), indicating the necessity of the aromatic group at this position. However, introduction of a nitrogen-containing aromatic group (**9**) resulted in a decrease in the reversal effect. Notably, the effects were minimal when OH-5 of lathyrol (**2**) was replaced with aromatic formyl (**10**) and propionyl (**12** and **13**) moieties, suggesting that the reversal activities were also associated with the size of the aromatic side chain at this position.

In Group II, thirteen derivatives containing two ester groups at C-3 and C-5 were investigated. Five compounds (**19**, **23**-**25** and **27**) exhibited higher MDR-modulating activities than VRP. Notably, compounds **19** and **25** were able to effectively reverse the sensitivity to ADR by 34.4 and 28.6 fold, respectively. As expected, compounds containing two aliphatic groups (**15**-**18**) exhibited a low reversal effect. Introduction of an acetyl group to OH-3 in **3** led to an enhanced reversal effect, as observed for **15**. The addition of a propionyl group in **10**, **11** and **14** increased the MDR reversal effect, as observed for **23**-**25**. The following trend in activity for the aromatic groups at C-5 was observed: 1-naphthylacetyl > phenylacetyl ≈ benzoyl. Although the 1-naphthylacetyl group was beneficial in **14** of Group I and **25** of Group II, the introduction together with

aromatic groups at C-3 in **14** resulted in a decreased reversal effect, as observed for **22** (R = 1-naphthylacetyl) and **26** (R = benzoyl). Similarly, replacement of the OH-3 with a phenylacetyl group in **11** reduced the MDR-modulating effect, as observed for compound **20**. Esterification of the OH-3 in compound **10** led to the active compounds **19**, **23** and **27**. The activity trend in terms of ester groups at C-3 is benzoyl > cinnamoyl > propionyl.

Compound **32** in Group V, bearing two acetyl moieties, exhibited greater reversal activity than VRP. Compared to **15**, **28** and **32**, which possess the same side chain, epoxidation of C-15 and C-12 (**32**) increased the activity; however, epoxidation of C-15 and C-11 (**28**) decreased the activity. An identical effect was observed for **18** and **34**, indicating that the epoxy ring in aliphatic-substituted compounds of Group V may be a favorable factor for the reversal effect. For the five-membered ring (Groups IV and V) derivatives, the aromatic-substituted compounds exhibited minimal activity. Compounds **29** and **35** exhibited much lower reversal activity than **19**, suggesting that the α, β-unsaturated ketone moiety is a key factor for the activity. Compounds **29**-**31** and **35**-**37** possessed an identical five-membered ring structure, with the exception of the methyl configuration at C-13, and these derivatives exhibited minimal MDR reversal activities. These results indicated that different configurations at C-13 did not greatly affect the MDR reversal activity.

Inhibition of Rh123 Efflux Mediated by P-gp. To confirm our hypothesis that *Euphorbia* factor L_3 derivatives inhibit the efflux activity of P-gp, compounds **14**, **19** and

25 were evaluated at several concentrations (2, 10 and 20 μM) using Rh123. Compared to the mean fluorescence intensity of VRP (170.0 at 20 μM), compounds **14**, **19** and **25** exhibited effective efflux inhibition of Rh123, with values ranging from 182.1 to 204.8 at 20 μM (Table 3). With increasing concentrations, the cumulative effect of compound **25** was rapidly enhanced, whereas compound **14** maintained a similar low level throughout the assessment. At low concentrations (2 μM), compound **19** exhibited a higher cumulative effect (FL-1 = 197.5) and remained unchanged (FL-1 = 204.8 at 10 and 20 μM) with increasing concentration. This dose-effect result suggested that an alternate mechanism may be involved in the activity of **19**.

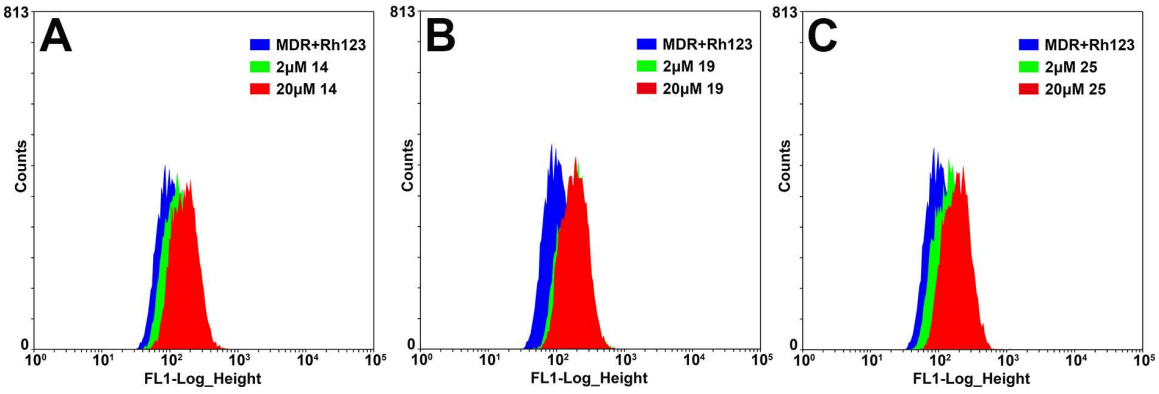

Figure 2. Inhibition effect of Rh123 efflux mediated by P-gp at 2 and 20 μM: (A) compound 14, (B) compound 19, and (C) compound 25.

Table 3. Inhibition Effect of Rh123 Efflux Mediated by P-gp

compd	concn (μM)	FSC[a]	SSC[b]	FL-1[c]	SD[d]	peak
14	2	134.9	96.3	141.1	61.6	131.1
	10	148.5	102.2	168.1	72.1	196.8
	20	138.7	94.2	182.1	77.1	205.9
19	2	146.8	102.7	197.5	90.8	215.4
	10	144.5	104.4	204.8	92.9	215.4
	20	148.1	102.0	204.8	88.2	196.8
25	2	138.5	94.8	149.4	66.3	143.5
	10	137.9	101.2	167.8	75.0	188.2
	20	131.4	100.9	204.6	89.3	235.8
MDR cells		142.5	100.6	108.1	43.9	87.3
PAR cells		112.8	81.1	217.5	76.7	215.4
VRP	20	137.4	92.2	170.0	66.7	157.1

[a]FSC: forward scatter count of cells. [b]SSC: side scatter count of cells. [c]FL-1: mean fluorescence intensity of the cells. [d] SD: standard deviation.

Physicochemical Properties and Linear Regression Analysis. Physicochemical parameters are summarized in Table S1, including molecular lipophilicity (Log*P*), bulkiness (MW, MV and ASA), H-bond features (HBA, HBD, and TPSA), molar refractivity (MR) and electrophilicity indices (ω, Table S2).[38,39] According to statistical analysis and the pharmacophore model, P-gp inhibitors or modulators are often hydrophobic, possess H-bond acceptors and tend to possess few H-bond donors.[40,41] All of the test compounds possess a greater number of H-bond acceptors (HBA = 4-5) than H-bond donors (HBD = 0-2). Compounds possessing a greater activity than VRP exhibited Log*P* > 4 and MW > 400 (except for **32**; Log*P* = 3.4) and were considered potential P-gp inhibitors or modulators.[42] For **10**-**14**, a single negative correlation with ω

(r^2 = 0.98) can be observed, suggesting a relationship between aromatic-substituted analogs in Group I and an electrostatic effect. Compounds **23**, **24**, and **25** in Group II, which differ in the ester group at C-5, exhibited a positive correlation with ASA (r^2 = 0.99), MW (r^2 = 0.96), MR (r^2 = 0.96), MV (r^2 = 0.93) and Log*P* (r^2 = 0.92). However, the MDR reversal activities of compounds **22**, **25** and **26**, which bear identical substituents at C-5, decreased with increasing Log*P* (r^2 = 0.92). Moreover, the analogs in Group II containing two aromatic groups with MW ≤ 568 and MV ≤ 541.6 were more active than VRP (**19**, **23**-**25** and **27**), and those with MW ≥ 570 and MV ≥ 547.7 were less active than VRP (**20**-**22** and **26**). This classification suggested that two bulky aromatic groups at C-3 and C-5 may not be well tolerated by P-gp. Compounds **19**, **23** and **27**, which contain identical benzoyl substituents at C-5, did not exhibit correlations with any parameters.

Molecular Modeling. The reported crystal structure of murine P-gp (PDB ID: 3G5U) is considered to represent the initial inward-facing stage of the transport cycle for drug binding. The structure of murine P-gp represents the highest resolution P-gp structure to date and was therefore selected for the homology modeling. The sequence alignment between human P-gp (UniProtKB: P08183) and murine P-gp using BLAST indicated 87% overall identity and 90% identity for all residues in the TMD (transmembrane domain).[43] A Ramachandran plot of the final homology model indicated that 85.7% of the residues were located in the most favored regions, 11.3% in the additionally allowed

regions, 2.1% in the generously allowed regions and 0.9% in the disallowed regions. No outliers in the TMD of P-gp were found, a feature that is important for estimation of the drug-binding ability (Figure 3A).

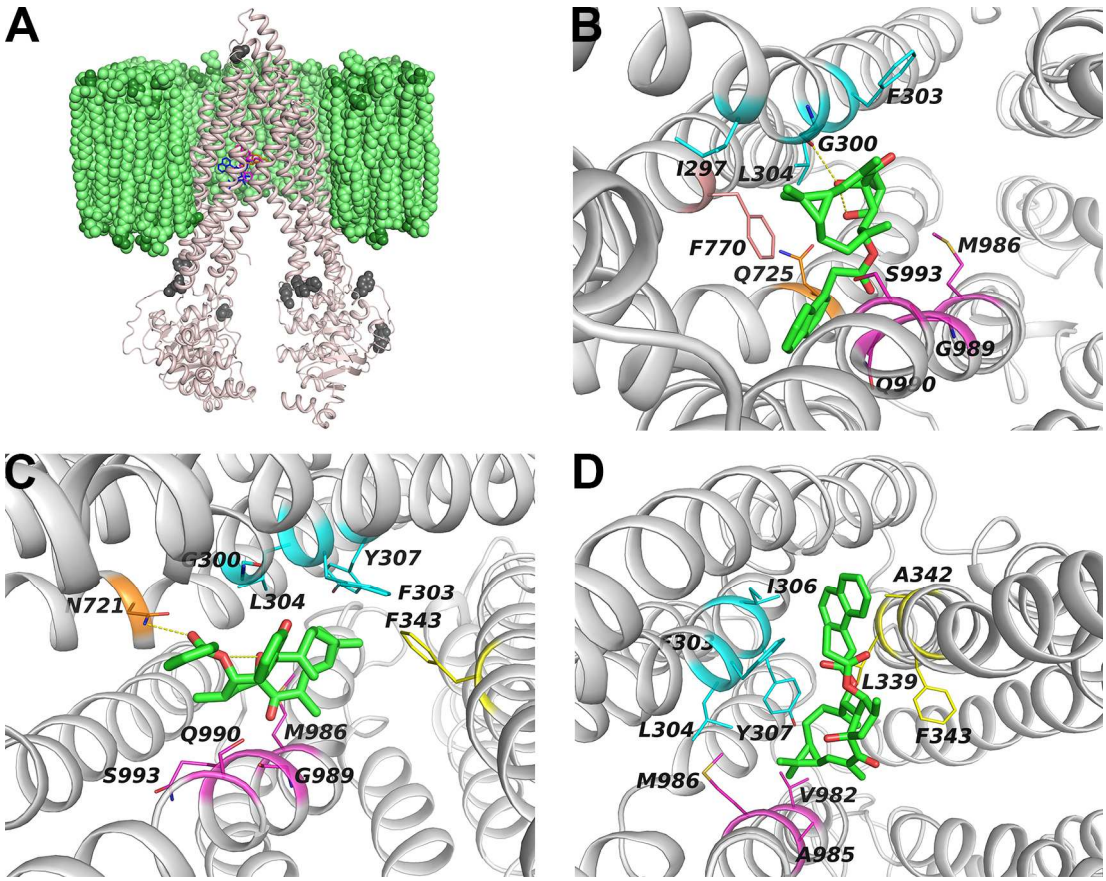

Figure 3. (A) Binding positions of 14, 19 and 25 in the homology model of human P-gp embedded in the POPC bilayer resulting from docking studies. The P-gp model was generated based on the template structure of the murine P-gp (PDB ID, 3G5U) and is portrayed as a cartoon. Outliers in the Ramachandran plot are indicated as dark gray spheres. The ligands are represented as colored sticks: 14, blue; 19, magenta; and 25, orange. POPC molecules are shown as light-green spheres. The phosphate groups are highlighted as forest green spheres. The front lipid molecules are not shown for clarity. All hydrogens are omitted. Binding modes of 14 (B), 19 (C) and 25 (D) obtained after 5-ns MD simulations. Carbon atoms of the ligands are

represented as green sticks. The hydrogen bonds are shown as yellow dashed lines. The P-gp receptor is shown as a gray cartoon. All hydrogens are omitted for clarity. Carbon atoms of interacting residues are depicted as colored sticks: TM5, cyan; TM6, yellow; TM7, orange; TM8, salmon; and TM12, magenta. Oxygen and nitrogen atoms of all stick representations are colored red and blue, respectively.

To further understand and characterize the interaction between the derivatives and the receptor, the three most promising ligands (**14**, **19** and **25**) were subjected to molecular docking with a homology model of P-gp. Because of the large and flexible drug-binding region of P-gp, the entire hydrophobic cavity was first considered as a binding pocket, and statistical results were subsequently used for the accurate docking. The substrates were finally located within the TMD regions of the binding pocket, as indicated by both biochemical and structural results.[14] The best conformation (Figure 3A) was used as the initial geometry for 5-ns MD calculations with explicit water and a POPC membrane.

The calculated binding free energies of **14**, **19** and **25** to P-gp are shown in Table 4. Compounds **14**, **19** and **25** were primarily stabilized by van der Waals interactions (ΔE_{vdw}), with values of -50.0, -51.8 and -51.0 kcal/mol, respectively. Nonpolar contributions, including ΔE_{vdw} and nonpolar solvation free energies (ΔG_{np}), were completely favorable for the binding process. For compounds **14** and **19**, a significant additional stabilization was gained through electrostatic interactions (ΔE_{elec} = -9.3 and -9.6 kcal/mol, respectively). Although the polar contribution (ΔE_{elec}) was favorable, the

polar solvation free energies (ΔG_{PB}) severely weakened binding of **14**, **19** and **25**. Therefore, the polar effect was not favorable for the binding of these lathyrol diterpenes to P-gp.

Table 4. Free Energy Analysis (kcal/mol) of the Binding of Compounds 14, 19 and 25 to P-gp.

compd	ΔE_{vdw} [a]	ΔE_{elec} [b]	ΔG_{PB} [c]	ΔG_{np} [d]	ΔG_{gas} [e]	ΔG_{solv} [f]	ΔG_{bind} [g]	SD [h]
14	-50.0	-9.3	29.5	-6.3	-59.3	23.2	-36.1	3.1
19	-51.8	-9.6	33.4	-6.9	-61.4	26.4	-34.9	3.4
25	-51.0	-3.3	22.0	-6.7	-54.3	15.3	-39.0	2.8

[a]ΔE_{vdw}: van der Waals interaction energy; [b]ΔE_{elec}: the electrostatic interaction energy; [c]ΔG_{PB}: the electrostatic contribution to the solvation free energy calculated by solving the linearised Poisson Boltzman (PB) equation; [d]ΔG_{np}: nonpolar contribution to the solvation free energy; [e]$\Delta G_{gas:}$ Gas phase energy ($\Delta E_{vdw}+\Delta E_{elec}$).; [f]$\Delta G_{solv}$: solvation free energy ($\Delta G_{np}+\Delta G_{PB}$); [g]$\Delta G_{bind}$: The final estimated binding free energy calculated from the terms above; [h]SD: standard deviation.

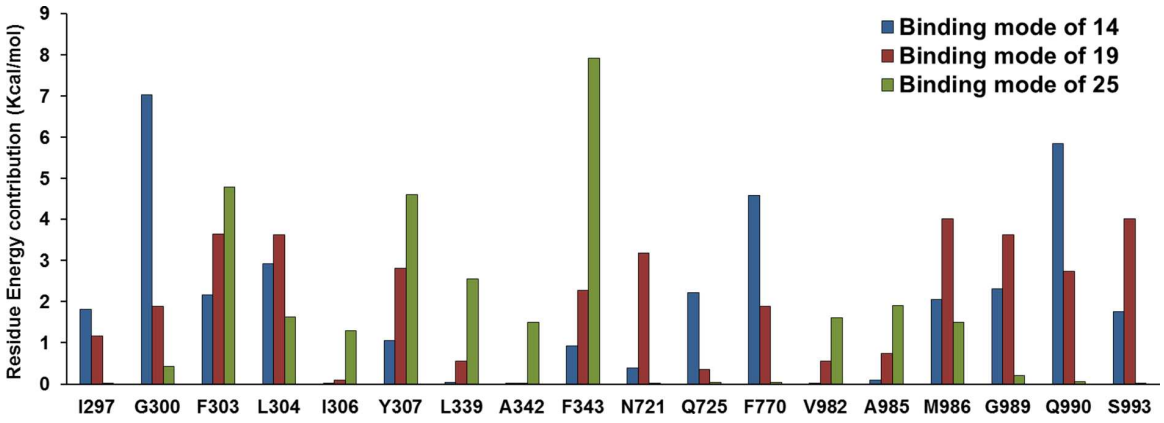

Figure 4. Energy contributions of the top 10 residues from ligand–residue interaction energy decomposition in the binding complexes of compounds 14, 19 and 25. Positive free energies (ignoring the negative sign) represent favorable binding.

As shown in Figures 3 and 4, the test structures exhibited a large number of nonbonding interactions, which primarily resulted from hydrophobic or aromatic residues in TMs 5, 6, 7, 8 and 12. Compound **14** was bound primarily by the interactions of residues Gly300 in TM5, Phe770 in TM8 and Gln990 in TM12 (Figures 3B, 4). The 1-naphthylacetyl group was inserted into the gap between TM7 and TM12 (Figure 3B), which is consistent with the speculation concerning the size of the side chain at C-5. A primary interaction was not found for compound **19**, and the binding free energies were primarily dispersed by Phe303 and Leu304 in TM5, Asn721 in TM7, and Met986, Gly989 and Ser993 in TM12. Two benzoyl groups of **19** protrude from the binding pocket (Figures 3C, 4), and this feature may be related to some extent to the lower flexibility of the benzoyl group. This feature was also found in compound **27**. For compound **25**, prominent hydrophobic interactions with Phe303 and Tyr307 in TM5 and Phe343 in TM6 (Figures 3D, 4) were observed. Furthermore, the 1-naphthylacetyl group is surrounded by TM5 and TM6 (Figure 3D), which may explain the hydrophobic trend with the reversal activities of **23**-**25.**

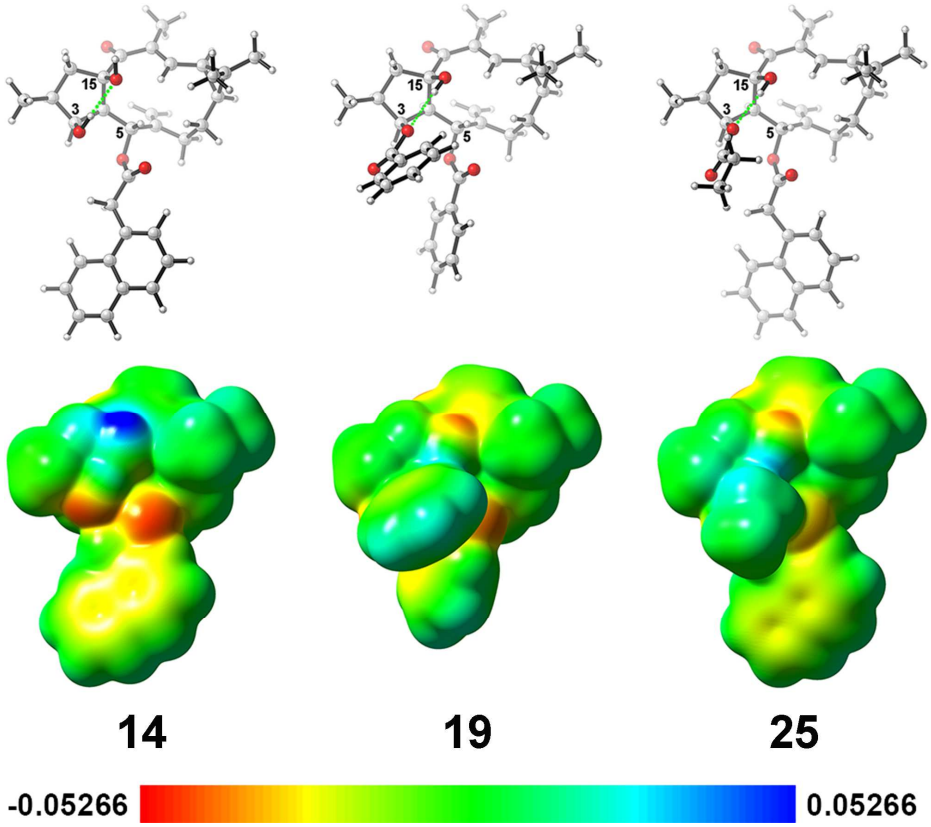

Figure 5. Electrostatic potential of 14, 19, and 25 mapped on the electron density surface. The scale of the electrostatic potential is negative (red) to positive (blue).

To evaluate the differences in the polar contributions among **14**, **19** and **25**, *ab initio* calculations were performed to map the electrostatic potential of the three compounds onto the respective molecular surfaces representing the electron densities (Figure 5). As observed for **14**, the potential H-donor at OH-15 was entirely electropositive, resulting from an intramolecular H-bond between OH-3 and O-15. For compound **14**, the most powerful polar interaction was the H-bond between OH-15 and Gly300. Most frames (71.5%) exhibited this H-bond effect with an average distance of 2.76 Å in the H-bond analysis. This strong bonding interaction (-3.699 kcal/mol) coupled with an

intramolecular H-bond greatly restricted the direction and position of **14** (Figure 6A, Table S3). Conversely, the hydrogen atom of OH-15 in compounds **19** and **25** revealed a considerably less positive charge due to the participation of OH-15 in an intramolecular H-bond with O-3. The electrostatic effect of **19** was influenced by an H-bond between the carbonyl of the benzoyl group at C-5 and Asn721 (ΔE_{elec} = -2.367) or between that at C-3 and Gly989 (ΔE_{elec} = -1.945) (Table S4). No effective H-bond interaction with residues was found in **25** during the MD simulation (Table S5). For compound **25**, the formation of an H-bond may be difficult due to the larger steric hindrance of the 1-naphthylacetyl group.

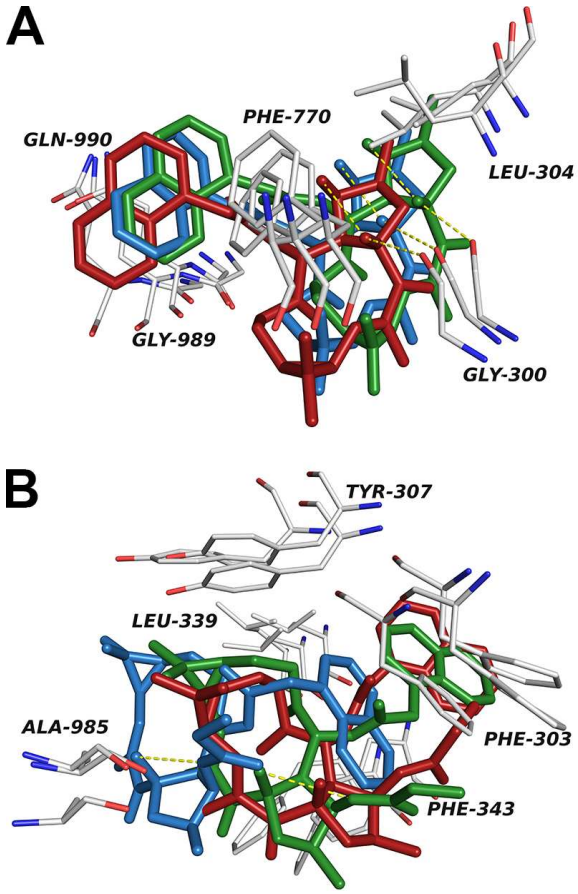

Figure 6. Superimposition of frames at 1, 3 and 5 ns in the MD trajectories of compounds 14 (A) and 25 (B). The strong interaction residues are shown as sticks: carbon, gray; oxygen, red; and nitrogen, blue. The ligands are depicted as colored sticks: 1 ns, sky blue; 3 ns, forest green; and 5 ns, crimson. All hydrogens are omitted for clarity.

The classic mechanism for P-gp transport proposes that P-gp undergoes large structural changes from an inward-facing to an outward-facing conformation during the catalytic cycle. As demonstrated by Cys cross-linking, the packing of the TM segments in P-gp is altered relative to the drug-free state through an induced-fit mechanism.[44] In this large and flexible drug-binding region, the continuous H-bond system in the complex with **14** should have constrained the adjustment ability of P-gp and ligand (Figure 6A). However, compound **25** was not fixed in the binding pocket during the MD simulation but interacted following variation of the flexible cavity. Even with the hydrophobic influence, the intramolecular H-bond in **25** gradually deconstructed to better adapt to the pocket (Figure 6B).

There are three contradictory details for the mechanism of **19** with P-gp: i) Compound **10** exhibited a dramatically low reversal effect but possesses an identical substituent at C-5 as **19**; ii) The efflux inhibition effect was not improved with increasing concentrations in the Rh123 efflux assay; and iii) The lowest binding free energy was inconsistent with the highest reversal fold. Therefore, we propose that the mechanism of action of compound

19 not only includes binding to the TMD but may include a synergistic mechanism, such as exerting a direct inhibitory effect on ATP hydrolysis, as previously reported.[45]

CONCLUSIONS

The hydroxyl groups at C-3 and C-5 were selectively acylated to investigate the effect of the acyl side chain on the lathyrol scaffold. Additionally, two new methods of epoxidation at OH-15 were used to demonstrate the function of the epoxy ring in this skeleton. Finally, 37 derivatives were newly designed and synthesized, varying in size, hydrophobicity and aromaticity. All synthesized derivatives were evaluated for MDR-modulating effects in MCF-7/ADR cells. In the lathyrol structure, the aromatic group at C-5 and the α, β-unsaturated ketone moiety are necessary to maintain the MDR reversal effect. In Group I, the size of the aromatic acetyl ester at C-5 was suitable for maximum activity. Furthermore, a low electrophilicity is favorable for the reversal activity. In Group II, the presence of a benzoyl group at C-5 increased the potency. Benzoylation of the OH-3 and OH-5 of lathyrol (**2**) produced the most active compound (**19**). Additionally, a combination of the propionyl group at C-3 and an aromatic group at C-5 led to an improvement in potency. Accordingly, compound **25** exhibited the second highest activity in this series. However, two bulky aromatic groups, such as phenylacetyl and 1-naphthylacetyl, at these two positions may not be well tolerated by P-gp and resulted in low activity. In Group V, the epoxidation of C-15 and C-11 increased the reversal activity of aliphatic substituted derivatives. Molecular modeling was used to

further demonstrate the binding modes of the derivatives with P-gp, including favorable nonpolar interactions and detrimental H-bond interactions. These results are applicable to similar skeletons of *Euphorbia* diterpenes to find chemosensitizers for future clinical development.

EXPERIMENTAL SECTION

General. The ESI-MS and high-resolution ESI-MS data were recorded on a Finnigan LCQ^{DECA} spectrometer and a Bruker Bio TOF Q spectrometer, respectively. Optical rotations were measured on an M341 polarimeter (PerkinElmer, USA). All reagents were purchased from commercial suppliers and used without further purification unless otherwise noted. Melting points were recorded on an X6 micro-melting point apparatus (Beijing Fukai, China) without correction. Thin-layer chromatography was performed using silica gel 60 GF_{254} precoated plates (0.20–0.25mm thickness) with a fluorescent indicator. Visualization on TLC was achieved by UV light (254 nm) and a typical TLC indication solution (10% sulfuric acid/ethanol solution). Column chromatography was performed on silica gel 90, 200-300 mesh and Sephadex LH-20 (70 μm, Amersham, Sweden). NMR spectra were recorded on a Bruker Avance 600 spectrometer (Bruker BioSpin, Switzerland) operating at 600 or 151 MHz for ^{1}H and ^{13}C, respectively. Spectra were assigned using appropriate COSY, DEPT, HMQC, and HMBC sequences. NMR chemical shifts are expressed in ppm (δ) referenced to the solvent used. Data are reported as follows: chemical shift, multiplicity, coupling constants (Hz) and integration. All final

compounds are >95% pure based on AQUITY Ultra Performance liquid chromatography (UPLC) system coupled to a photodiode array detector (PDA) (Waters Corporation, Milford, MA, USA).

Plant Material. Seeds of *Euphorbia Lathyris* were collected in Sichuan province, P. R. China, and identified by Xin Chao Long, information center of Sinotcm Corporation, Chengdu. A voucher specimen (No. 20110812-021) was deposited at Chengdu Institute of Biology, Chinese Academy of Sciences.

Extraction and Isolation. The powdered seeds of *E. lathyris* (10 kg) were exhaustively extracted with 95% ethanol/acetone (5:1) at room temperature (4 × 30 L). Following evaporation of the solvent under vacuum, the crude oil (3.5 kg) was subjected to column chromatography over silica gel using petrol/EtOAc (20:1) to remove a large quantity of lipophilic oil. The residue was chromatographed on silica gel using a petrol/EtOAc stepwise elution to afford 5 fractions according to thin-layer chromatography. Fraction 2 was applied to silica gel using a petrol/EtOAc stepwise elution and then subjected to Sephadex LH-20 using MeOH/H_2O to afford *Euphorbia* factor L_3 (22.6 g).

***Euphorbia* factor L_3, *(12E,2S,3S,4R,5R,9S,11R,15R)-5,15-Diacetoxy-3-benzoyloxylathyra-6(17),12-dien-14-one* (1).** White powder; mp 152–154 °C; ESI-MS *m/z* 545 $[M+Na]^+$; IR (KBr, ν_{max}, cm^{-1}) 3452, 2927, 2858, 1739, 1714, 1651, 1622, 1452, 1369, 1277, 1223, 1110, 1068, 1008, 713; ^1H NMR (600 MHz, $CDCl_3$) δ 6.54 (d, J = 11.5 Hz, 1H, H-12), 6.21 (d, J = 10.0 Hz, 1H, H-5), 5.82 (d, J = 3.2 Hz, 1H, H-3), 5.01 (s,

1H, H-17a), 4.78 (s, 1H, H-17b), 3.53 (dd, *J* = 14.2, 8.4 Hz, 1H, H-1*α*), 2.90 (dd, *J* = 9.8, 3.4 Hz, 1H, H-4), 2.40–2.30 (m, 1H, H-2), 2.23–2.16 (m, 1H, H-7*α*), 2.05–1.98 (m, 1H, H-7*β*), 1.98–1.91 (m, 1H, H-8*α*), 1.79–1.71 (m, 1H, H-8*β*), 1.72 (s, 3H, H-20), 1.70–1.64 (m, 1H, H-1*β*), 1.41 (dd, *J* = 11.2, 8.2 Hz, 1H, H-11), 1.18 (s, 3H, H-18), 1.17 (s, 3H, H-19), 1.20–1.13 (m, 1H, H-9), 0.94 (d, *J* = 6.6 Hz, 3H, H-16), 3-*O*-benzoyl: 8.03 (d, *J* = 7.6 Hz, 2H), 7.58 (t, *J* = 7.6 Hz, 1H), 7.45 (t, *J* = 7.6 Hz, 2H), 5-OAc: 1.82 (s, 3H), 15-OAc: 2.21 (s, 3H); ^{13}C NMR (151 MHz, $CDCl_3$) *δ* 196.7 (C-14), 146.5 (C-12), 144.6 (C-6), 134.2 (C-13), 115.4 (C-17), 92.5 (C-15), 80.9 (C-3), 65.5 (C-5), 52.2 (C-4), 48.6 (C-1), 37.9 (C-2), 35.4 (C-9), 35.0 (C-7), 29.0 (C-19), 28.5 (C-11), 25.3 (C-10), 21.7 (C-8), 16.8 (C-18), 14.2 (C-16), 12.4 (C-20), 3-*O*-benzoyl: 166.1, 133.1, 130.1, 129.6, 129.6, 128.3, 128.3, 5-OAc: 169.7, 22.0, 15-OAc: 170.1, 20.9.

(12E,2S,3S,4R,5R,9S,11R,15R)-Lathyra-6(17),12-dien-3,5,15-triol-14-one **(2).** A suspension of **1** (5 g, 9.6 mmol) in 5% KOH and MeOH (100 mL) was stirred at room temperature for 24 h. Further purification was performed by flash column chromatography (petroleum ether/EtOAc = 4:1) to afford **2** as a colorless crystal (2.9 g, yield 89 %). IR (KBr, v_{max}, cm^{-1}) 3415, 2954, 2925, 2861, 1622, 1445, 1269, 1146, 1048, 1015, 909; ESI-MS *m/z* 357 [M+Na]$^+$; mp: 158–160 °C; ^{1}H NMR (600 MHz, acetone-d_6) *δ* 7.10 (d, *J* = 11.4 Hz, 1H, H-12), 4.79 (s, 1H, H-17a), 4.68 (s, 1H, H-17b), 4.70–4.64 (m, 1H, H-5), 4.45 (s, 1H, OH-15), 4.33 (d, *J* = 2.8 Hz, 1H, H-3), 4.03 (s, 1H, OH-3), 3.94 (d, *J* = 6.8 Hz, 1H, OH-5), 3.04 (dd, *J* = 13.4, 9.1 Hz, 1H, H-1*α*), 2.69–2.60 (m, 1H, H-7*α*),

2.24 (dd, J = 7.7, 3.4 Hz, 1H, H-4), 2.02–1.94 (m, 2H, H-7β, H-2), 1.92–1.82 (m, 1H, H-8α), 1.70 (d, J = 0.7 Hz, 3H, H-20), 1.63 (dd, J = 13.4, 11.0 Hz, 1H, H-1β), 1.59–1.50 (m, 1H, H-8β), 1.46 (dd, J = 11.5, 8.6 Hz, 1H, H-11), 1.22–1.16 (m, 1H, H-9), 1.15 (s, 3H, H-18), 1.12 (s, 3H, H-19), 1.08 (d, J = 6.8 Hz, 3H, H-16); ^{13}C NMR (151 MHz, acetone-d_6) δ 202.4 (C-14), 150.8 (C-12), 147.7 (C-6), 135.8 (C-13), 111.1 (C-17), 89.9 (C-15), 79.7 (C-3), 67.7 (C-5), 55.7 (C-4), 49.4 (C-1), 38.4 (C-2), 36.2 (C-7), 35.8 (C-9), 29.2 (C-19), 28.9 (C-11), 25.3 (C-10), 23.1 (C-8), 16.5 (C-18), 14.7 (C-16), 13.2 (C-20).

(12E,2S,3S,4R,5R,9S,11R,15R)-5-Acetoxylathyra-6(17),12-dien-3,15-diol-14-one **(3).** To a 0 °C solution of acetic acid (13 μL, 0.23 mmol), EDCI (44 mg, 0.23 mmol) and DMAP (4 mg, 0.03 mmol) in CH_2Cl_2 (5 mL) was added **2** (70 mg, 0.21 mmol). The mixture was allowed to warm to room temperature and stirred for 48 h. Further purification was performed by flash column chromatography (petroleum ether/EtOAc = 8:1) to give **3** as a colorless crystal (52 mg, yield 75%). HRMS-ESI-TOF *m/z* calcd for $C_{22}H_{32}O_5Na$ $[M+Na]^+$ 399.2130, found 399.2142; mp: 141–143 °C; $[\alpha]_D^{20}$ +170° (*c* 0.1, acetone); ^{1}H NMR (600 MHz, acetone-d_6) δ 7.46 (br s, 1H, H-12), 6.08 (d, J = 10.4 Hz, 1H, H-5), 4.89 (s, 1H, H-17a), 4.67 (s, 1H, H-17b), 4.58 (s, 1H, OH-15), 4.22–4.15 (m, 1H, H-3), 3.79 (br s, 1H, OH-3), 3.17 (dd, J = 13.4, 10.0 Hz, 1H, H-1α), 2.44 (dd, J = 10.4, 3.0 Hz, 1H, H-4), 2.30 (dd, J = 13.8, 6.7 Hz, 1H, H-7α), 2.12–1.99 (m, 1H, H-2), 2.04–2.00 (m, 1H, H-7β), 1.91–1.75 (m, 2H, H-8α, H-8β), 1.66 (s, 3H, H-20), 1.57 (dd, J = 13.8, 10.4 Hz, 1H, H-1β), 1.48 (dd, J = 11.7, 8.6 Hz, 1H, H-11), 1.25–1.18 (m, 1H,

H-9), 1.17 (s, 3H, H-18), 1.17 (s, 3H, H-19), 1.07 (d, J = 6.8 Hz, 3H, H-16), 5-OAc: 1.97 (s, 3H); ^{13}C NMR (151 MHz, acetone-d_6) δ 200.7 (C-14), 151.1 (C-12), 146.8 (C-6), 135.7 (C-13), 114.2 (C-17), 90.5 (C-15), 80.3 (C-3), 68.6 (C-5), 55.0 (C-4), 50.1 (C-1), 38.6 (C-2), 37.0 (C-9), 35.5 (C-7), 29.5 (C-11), 29.2 (C-19), 26.0 (C-10), 22.5 (C-8), 16.7 (C-18), 15.0 (C-16), 13.0 (C-20), 5-OAc: 171.0, 21.2.

(12E,2S,3S,4R,5R,9S,11R,15R)-5-Propionyloxylathyra-6(17),12-dien-3,15-diol-14-one **(4).** Starting from propanoic acid, the title compound was prepared following the same procedure used for the synthesis of **3** and was obtained as a white amorphous solid (yield 74%). HRMS-ESI-TOF *m/z* calcd for $C_{23}H_{34}NaO_5$ $[M+Na]^+$ 413.2308, found 413.2298; $[\alpha]_D^{20}$ +226° (*c* 2.4, acetone); ^{1}H NMR (600 MHz, acetone-d_6) δ 7.46 (br s, 1H, H-12), 6.10 (d, J = 10.4 Hz, 1H, H-5), 4.88 (s, 1H, H-17a), 4.67 (s, 1H, H-17b), 4.60 (s, 1H, OH-15), 4.19 (dt, J = 6.1, 3.1 Hz, 1H, H-3), 3.75 (br s, 1H, OH-3), 3.16 (dd, J = 13.4, 10.2 Hz, 1H, H-1α), 2.45 (dd, J = 10.4, 3.0 Hz, 1H, H-4), 2.35–2.23 (m, 1H, H-7α), 2.12–2.06 (m, 1H, H-2), 2.04–1.99 (m, 1H, H-7β), 1.92–1.77 (m, 2H, H-8α, H-8β), 1.66 (s, 3H, H-20), 1.57 (dd, J = 13.8, 10.4 Hz, 1H, H-1β), 1.48 (dd, J = 11.7, 8.6 Hz, 1H, H-11), 1.25–1.18 (m, 1H, H-9), 1.17 (s, 3H, H-18), 1.17 (s, 3H, H-19), 1.06 (d, J = 6.8 Hz, 3H, H-16), 5-*O*-propionyl: 2.35–2.23 (m, 2H), 1.06 (t, J = 7.5 Hz, 3H); ^{13}C NMR (151 MHz, acetone-d_6) δ 200.8 (C-14), 150.9 (C-12), 146.9 (C-6), 135.7 (C-13), 114.1 (C-17), 90.6 (C-15), 80.3 (C-3), 68.6 (C-5), 55.1 (C-4), 50.1 (C-1), 38.7 (C-2), 37.0 (C-9), 35.5

(C-7), 29.5 (C-11), 29.2 (C-19), 26.0 (C-10), 22.6 (C-8), 16.7 (C-18), 15.1 (C-16), 13.1 (C-20), 5-*O*-propionyl: 174.3, 28.2, 9.5.

***(12E,2S,3S,4R,5R,9S,11R,15R)-5-Valeryloxylathyra-6(17),12-dien-3,15-diol-14-one* (5).** Starting from pentanoic acid, the title compound was prepared following the same procedure used for the synthesis of **3** and was obtained as a syrup (yield 68%). HRMS-ESI-TOF *m/z* calcd for $C_{25}H_{38}O_5Na$ $[M+Na]^+$ 441.2608, found 441.2611; $[\alpha]_D^{20}$ +196° (*c* 1.0, acetone); ^{1}H NMR (600 MHz, acetone-d_6) δ 7.45 (br s, 1H, H-12), 6.10 (d, J = 10.4 Hz, 1H, H-5), 4.89 (s, 1H, H-17a), 4.68 (s, 1H, H-17b), 4.62 (s, 1H, OH-15), 4.18 (dt, J = 6.1, 3.2 Hz, 1H, H-3), 3.72 (br s, 1H, OH-3), 3.16 (dd, J = 13.1, 10.4 Hz, 1H, H-1α), 2.45 (dd, J = 10.4, 3.0 Hz, 1H, H-4), 2.33–2.24 (m, 1H, H-7α), 2.12–2.06 (m, 1H, H-2), 2.04–1.98 (m, 1H, H-7β), 1.92–1.77 (m, 2H, H-8α, H-8β), 1.66 (s, 3H, H-20), 1.61–1.52 (m, 1H, H-1β), 1.49 (dd, J = 11.4, 8.6 Hz, 1H, H-11), 1.25–1.19 (m, 1H, H-9), 1.17 (s, 3H, H-18), 1.17 (s, 3H, H-19), 1.07 (d, J = 6.8 Hz, 3H, H-16), 5-*O*-valeryl: 2.33–2.24 (m, 2H), 1.61–1.52 (m, 2H), 1.38–1.28 (m, 2H), 0.89 (t, J = 7.4 Hz, 3H); ^{13}C NMR (151 MHz, acetone-d_6) δ 200.9 (C-14), 150.9 (C-12), 146.9 (C-6), 135.8 (C-13), 114.1 (C-17), 90.5 (C-15), 80.3 (C-3), 68.6 (C-5), 55.1 (C-4), 50.1 (C-1), 38.7 (C-2), 37.0 (C-9), 35.5 (C-7), 29.5 (C-11), 29.2 (C-19), 26.1 (C-10), 22.6 (C-8), 16.7 (C-18), 15.1 (C-16), 13.1 (C-20), 5-*O*-valeryl: 173.7, 34.7, 27.9, 23.1, 14.2.

***(12E,2S,3S,4R,5R,9S,11R,15R)-5-Hexanoyloxylathyra-6(17),12-dien-3,15-diol-14-one* (6).** Starting from hexanoic acid, the title compound was prepared following the same

procedure used for the synthesis of **3** and was obtained as a syrup (yield 74%). HRMS-ESI-TOF *m/z* calcd for $C_{26}H_{40}O_5Na$ $[M+Na]^+$ 455.2751, found 455.2768; $[\alpha]_D^{20}$ +153° (*c* 1.0, acetone); ^1H NMR (600 MHz, acetone-d_6) δ 7.46 (br s, 1H, H-12), 6.10 (d, J = 10.4 Hz, 1H, H-5), 4.89 (s, 1H, H-17a), 4.68 (s, 1H, H-17b), 4.63 (s, 1H, OH-15), 4.21–4.15 (m, 1H, H-3), 3.72 (br s, 1H, OH-3), 3.16 (dd, J = 12.7, 10.9 Hz, 1H, H-1α), 2.45 (dd, J = 10.4, 2.8 Hz, 1H, H-4), 2.34–2.23 (m, 1H, H-7α), 2.13–2.06 (m, 1H, H-2), 2.04–1.99 (m, 1H, H-7β), 1.93–1.77 (m, 2H, H-8α, H-8β), 1.66 (s, 3H, H-20), 1.62–1.53 (m, 1H, H-1β), 1.49 (dd, J = 11.7, 8.7 Hz, 1H, H-11), 1.26–1.19 (m, 1H, H-9), 1.17 (s, 3H, H-18), 1.17 (s, 3H, H-19), 1.07 (d, J = 6.8 Hz, 3H, H-16), 5-*O*-hexanoyl: 2.34–2.23 (m, 2H), 1.62–1.53 (m, 2H), 1.36–1.26 (m, 4H), 0.88 (t, J = 6.7 Hz, 3H); ^{13}C NMR (151 MHz, acetone-d_6) δ 200.8 (C-14), 151.0 (C-12), 146.9 (C-6), 135.8 (C-13), 114.2 (C-17), 90.6 (C-15), 80.3 (C-3), 68.6 (C-5), 55.1 (C-4), 50.1 (C-1), 38.7 (C-2), 37.0 (C-9), 35.5 (C-7), 29.5 (C-11), 29.2 (C-19), 26.1 (C-10), 22.6 (C-8), 16.7 (C-18), 15.1 (C-16), 13.1 (C-20), 5-*O*-hexanoyl: 173.7, 35.0, 32.2, 25.5, 23.2, 14.4.

(12E,2S,3S,4R,5R,9S,11R,15R)-5-Isobutyryloxylathyra-6(17),12-dien-3,15-diol-14-one **(7).** Starting from isobutyric acid, the title compound was prepared following the same procedure used for the synthesis of **3** and was obtained as a white amorphous solid (yield 65%). HRMS-ESI-TOF *m/z* calcd for $C_{24}H_{36}O_5Na$ $[M+Na]^+$ 427.2454, found 427.2455; $[\alpha]_D^{20}$ +344° (*c* 0.1, acetone); ^1H NMR (600 MHz, acetone-d_6) δ 7.43 (br s, 1H, H-12), 6.10 (d, J = 10.3 Hz, 1H, H-5), 4.89 (s, 1H, H-17a), 4.69 (s, 1H, H-17b), 4.66 (s, 1H,

OH-15), 4.20 (dt, *J* = 6.1, 3.2 Hz, 1H, H-3), 3.66 (br s, 1H, OH-3), 3.15 (dd, *J* = 13.1, 10.6 Hz, 1H, H-1*α*), 2.47 (dd, *J* = 10.3, 2.9 Hz, 1H, H-4), 2.26 (dd, *J* = 14.1, 7.1 Hz, 1H, H-7*α*), 2.14–2.06 (m, 1H, H-2), 2.04–1.99 (m, 1H, H-7*β*), 1.92–1.77 (m, 2H, H-8*α*, H-8*β*), 1.67 (s, 3H, H-20), 1.57 (dd, *J* = 13.9, 10.3 Hz, 1H, H-1*β*), 1.49 (dd, *J* = 11.7, 8.6 Hz, 1H, H-11), 1.25–1.19 (m, 1H, H-9), 1.17 (s, 3H, H-18), 1.17 (s, 3H, H-19), 1.07 (d, *J* = 6.8 Hz, 3H, H-16), 5-*O*-isobutyryl: 2.55–2.48 (m, 1H), 1.12 (d, *J* = 2.5 Hz, 3H), 1.11 (d, *J* = 2.5 Hz, 3H); ^{13}C NMR (151 MHz, acetone-*d*$_6$) *δ* 201.0 (C-14), 150.8 (C-12), 146.9 (C-6), 135.8 (C-13), 114.1 (C-17), 90.6 (C-15), 80.1 (C-3), 68.6 (C-5), 55.1 (C-4), 50.1 (C-1), 38.8 (C-2), 37.0 (C-9), 35.4 (C-7), 29.5 (C-11), 29.2 (C-19), 26.0 (C-10), 22.6 (C-8), 16.7 (C-18), 15.1 (C-16), 13.1 (C-20), 5-*O*-isobutyryl: 176.7, 34.9, 19.5, 19.2.

(12E,2S,3S,4R,5R,9S,11R,15R)-5-Isovaleryloxylathyra-6(17),12-dien-3,15-diol-14-one **(8).** Starting from isovaleric acid, the title compound was prepared following the same procedure used for the synthesis of **3** and was obtained as a white amorphous solid (yield 80%). HRMS-ESI-TOF *m/z* calcd for $C_{25}H_{38}O_5Na$ $[M+Na]^+$ 441.2621, found 441.2611; $[\alpha]_D^{20}$ +205° (*c* 0.1, acetone); ^{1}H NMR (600 MHz, acetone-*d*$_6$) *δ* 7.45 (br s, 1H, H-12), 6.09 (d, *J* = 10.4 Hz, 1H, H-5), 4.89 (s, 1H, H-17a), 4.68 (s, 1H, H-17b), 4.65 (s, 1H, OH-15), 4.20–4.14 (m, 1H, H-3), 3.69 (br s, 1H, OH-3), 3.21–3.08 (m, 1H, H-1*α*), 2.45 (dd, *J* = 10.5, 2.8 Hz, 1H, H-4), 2.31 (dd, *J* = 14.1, 7.1 Hz, 1H, H-7*α*), 2.12–2.00 (m, 2H, H-2, H-7*β*), 1.93–1.77 (m, 2H, H-8*α*, H-8*β*), 1.66 (s, 3H, H-20), 1.57 (dd, *J* = 13.8, 10.4 Hz, 1H, H-1*β*), 1.49 (dd, *J* = 11.7, 8.7 Hz, 1H, H-11), 1.26–1.19 (m, 1H, H-9), 1.17 (s,

3H, H-18), 1.17 (s, 3H, H-19), 1.06 (d, J = 6.8 Hz, 3H, H-16), 5-*O*-isovaleryl: 2.22–2.12 (m, 2H), 2.12–2.00 (m, 1H), 0.94 (d, J = 1.6 Hz, 3H), 0.92 (d, J = 1.5 Hz, 3H); ^{13}C NMR (151 MHz, acetone-d_6) δ 200.9 (C-14), 150.9 (C-12), 146.8 (C-6), 135.7 (C-13), 114.2 (C-17), 90.5 (C-15), 80.2 (C-3), 68.5 (C-5), 55.1 (C-4), 50.1 (C-1), 38.7 (C-2), 37.0 (C-9), 35.4 (C-7), 29.4 (C-11), 29.2 (C-19), 26.0 (C-10), 22.5 (C-8), 16.7 (C-18), 15.1 (C-16), 13.1 (C-20), 5-*O*-isovaleryl: 173.0, 44.1, 26.3, 22.9, 22.8.

***(12E,2S,3S,4R,5R,9S,11R,15R)-5-Nicotinoyloxylathyra-6(17),12-dien-3,15-diol-14-one* (9).** Starting from nicotinic acid, the title compound was prepared following the same procedure used for the synthesis of **3** and was obtained as a white amorphous solid (yield 31%). HRMS-ESI-TOF *m/z* calcd for $C_{26}H_{33}NO_5Na$ $[M+Na]^+$ 462.2257, found 441.2251; $[\alpha]_D^{20}$ +266° (*c* 0.1, acetone); ^{1}H NMR (600 MHz, acetone-d_6) δ 7.53 (br s, 1H, H-12), 6.42 (d, J = 10.4 Hz, 1H, H-5), 4.99 (s, 1H, H-17a), 4.83 (s, 1H, H-17b), 4.67 (s, 1H, OH-15), 4.32 (dt, J = 6.1, 3.2 Hz, 1H, H-3), 3.98 (br s, 1H, OH-3), 3.20 (dd, J = 12.9, 10.5 Hz, 1H, H-1α), 2.66 (dd, J = 10.4, 2.9 Hz, 1H, H-4), 2.41–2.33 (m, 1H, H-7α), 2.19–2.07 (m, 2H, H-2, H-7β), 1.99–1.90 (m, 2H, H-8α, H-8β), 1.70 (s, 3H, H-20), 1.60 (dd, J = 13.9, 10.4 Hz, 1H, H-1β), 1.53 (dd, J = 11.8, 8.6 Hz, 1H, H-11), 1.30–1.23 (m, 1H, H-9), 1.22 (s, 3H, H-18), 1.19 (s, 3H, H-19), 1.04 (d, J = 6.9 Hz, 3H, H-16), 5-*O*-nicotinoyl: 9.12 (d, J = 1.4 Hz, 1H), 8.75 (dd, J = 4.7, 1.4 Hz, 1H), 8.30 (dt, J = 7.9, 1.9 Hz, 1H), 7.50 (dd, J = 7.9, 4.9 Hz, 1H); ^{13}C NMR (151 MHz, acetone-d_6) δ 200.8 (C-14), 150.8 (C-12), 146.4 (C-6), 135.8 (C-13), 115.0 (C-17), 90.7 (C-15), 80.3 (C-3),

70.2 (C-5), 55.0 (C-4), 50.0 (C-1), 38.8 (C-2), 37.0 (C-9), 35.4 (C-7), 29.5 (C-11), 29.2 (C-19), 26.1 (C-10), 22.6 (C-8), 16.7 (C-18), 15.0 (C-16), 13.1 (C-20), 5-*O*-nicotinoyl: 165.6, 154.3, 151.6, 137.8, 127.7, 124.6.

(12E,2S,3S,4R,5R,9S,11R,15R)-5-Benzoyloxylathyra-6(17),12-dien-3,15-diol-14-one **(10).** To a 0 °C solution of **2** (80 mg, 0.24 mmol) in CH_2Cl_2 (5 mL) were sequentially added DMAP (4 mg, 0.03 mmol), Et_3N (107 μL, 0.77 mmol), and benzoic anhydride (224 mg, 0.99 mmol) under argon atmosphere. The reaction was warmed to room temperature gradually and stirred for 24 h. Further purification was performed by flash column chromatography (petroleum ether/EtOAc = 14:1) to give **9** as a white amorphous solid (70 mg, yield 66%). HRMS-ESI-TOF *m/z* calcd for $C_{27}H_{34}O_5Na$ $[M+Na]^+$ 461.2290, found 441.2298; $[\alpha]_D^{20}$ +251° (*c* 1.5, acetone); ^{1}H NMR (600 MHz, acetone-d_6) δ 7.68–7.32 (m, 1H, H-12), 6.37 (d, *J* = 10.3 Hz, 1H, H-5), 4.96 (s, 1H, H-17a), 4.81 (s, 1H, H-17b), 4.67 (s, 1H, OH-15), 4.30 (dt, *J* = 5.8, 3.0 Hz, 1H, H-3), 3.91 (br s, 1H, OH-3), 3.24–3.13 (m, 1H, H-1α), 2.64 (dd, *J* = 10.3, 2.8 Hz, 1H, H-4), 2.39–2.31 (m, 1H, H-7α), 2.18–2.06 (m, 2H, H-2, H-7β), 1.98–1.88 (m, 2H, H-8α, H-8β), 1.70 (s, 3H, H-20), 1.60 (dd, *J* = 13.9, 10.3 Hz, 1H, H-1β), 1.52 (dd, *J* = 11.7, 8.6 Hz, 1H, H-11), 1.34–1.22 (m, 1H, H-9), 1.22 (s, 3H, H-18), 1.19 (s, 3H, H-19), 1.05 (d, *J* = 6.8 Hz, 3H, H-16), 5-*O*-benzoyl: 8.01 (d, *J* = 8.3 Hz, 2H), 7.61 (t, *J* = 7.4 Hz, 1H), 7.49 (t, *J* = 7.7 Hz, 2H); ^{13}C NMR (151 MHz, acetone-d_6) δ 201.0 (C-14), 150.8 (C-12), 146.7 (C-6), 135.8 (C-13), 114.6 (C-17), 90.7 (C-15), 80.2 (C-3), 69.7 (C-5), 55.2 (C-4), 50.1 (C-1), 38.8 (C-2), 37.0

(C-9), 35.6 (C-7), 29.5 (C-11), 29.2 (C-19), 26.1 (C-10), 22.6 (C-8), 16.7 (C-18), 15.0 (C-16), 13.1 (C-20), 5-*O*-benzoyl: 166.6, 133.8, 132.0, 130.5, 130.5, 129.5, 129.5.

(12E,2S,3S,4R,5R,9S,11R,15R)-5-Phenylacetyloxylathyra-6(17),12-dien-3,15-diol-14-one **(11).** Starting from phenylacetic acid, the title compound was prepared following the same procedure used for the synthesis of **3** and was obtained as a white amorphous solid (yield 72%). HRMS-ESI-TOF *m/z* calcd for $C_{28}H_{36}O_5Na$ $[M+Na]^+$ 475.2446, found 441.2455; $[\alpha]_D^{20}$ +211° (*c* 0.9, acetone); ^{1}H NMR (600 MHz, acetone-d_6) δ 7.43 (br s, 1H, H-12), 6.12 (d, *J* = 10.4 Hz, 1H, H-5), 4.87 (s, 1H, H-17a), 4.67 (s, 1H, H-17b), 4.60 (s, 1H, OH-15), 4.15–4.07 (m, 1H, H-3), 3.62 (s, 1H, OH-3), 3.20–3.11 (m, 1H, H-1α), 2.44 (dd, *J* = 10.4, 3.1 Hz, 1H, H-4), 2.21 (dd, *J* = 13.8, 6.7 Hz, 1H, H-7α), 2.10–2.00 (m, 1H, H-2), 2.00–1.90 (m, 1H, H-7β), 1.88–1.73 (m, 2H, H-8α, H-8β), 1.65 (s, 3H, H-20), 1.56 (dd, *J* = 13.9, 10.4 Hz, 1H, H-1β), 1.47 (dd, *J* = 11.8, 8.6 Hz, 1H, H-11), 1.22–1.16 (m, 1H, H-9), 1.15 (s, 3H, H-18), 1.15 (s, 3H, H-19), 1.06 (d, *J* = 6.8 Hz, 3H, H-16), 5-*O*-phenylacetyl: 7.33–7.19 (m, 5H), 3.64 (s, 2H); ^{13}C NMR (151 MHz, acetone-d_6) δ 200.8 (C-14), 150.5 (C-12), 146.6 (C-6), 135.7 (C-13), 114.3 (C-17), 90.6 (C-15), 80.2 (C-3), 69.2 (C-5), 55.0 (C-4), 50.0 (C-1), 38.7 (C-2), 37.0 (C-9), 35.3 (C-7), 29.5 (C-11), 29.2 (C-19), 26.0 (C-10), 22.5 (C-8), 16.7 (C-18), 15.1 (C-16), 13.1 (C-20), 5-*O*-phenylacetyl: 171.8, 135.9, 130.5, 130.5, 129.3, 129.3, 127.7, 41.8.

(12E,2S,3S,4R,5R,9S,11R,15R)-5-Phenylpropionyloxylathyra-6(17),12-dien-3,15-diol-14-one **(12).** Starting from phenylpropionic acid, the title compound was prepared

following the same procedure used for the synthesis of **3** and was obtained as a syrup (yield 72%). HRMS-ESI-TOF *m/z* calcd for $C_{29}H_{38}O_5Na$ $[M+Na]^+$ 489.2610, found 489.2611; $[\alpha]_D^{20}$ +139° (*c* 6.5, acetone); ^{1}H NMR (600 MHz, acetone-d_6) δ 7.47 (br s, 1H, H-12), 6.11 (d, *J* = 10.5 Hz, 1H, H-5), 4.87 (s, 1H, H-17a), 4.67 (s, 1H, H-17b), 4.58 (s, 1H, OH-15), 4.12 (br s, 1H, H-3), 3.65 (br s, 1H, OH-3), 3.20–3.12 (m, 1H, H-1α), 2.44 (dd, *J* = 10.5, 2.9 Hz, 1H, H-4), 2.16 (dd, *J* = 14.1, 6.5 Hz, 1H, H-7α), 2.11–2.00 (m, 1H, H-2), 2.00–1.92 (m, 1H, H-7β), 1.88–1.77 (m, 2H, H-8α, H-8β), 1.65 (s, 3H, H-20), 1.56 (dd, *J* = 13.8, 10.4 Hz, 1H, H-1β), 1.48 (dd, *J* = 11.7, 8.7 Hz, 1H, H-11), 1.23–1.18 (m, 1H, H-9), 1.17 (s, 3H, H-18), 1.17 (s, 3H, H-19), 1.05 (d, *J* = 6.9 Hz, 3H, H-16), 5-*O*-phenylpropionyl: 7.34–7.10 (m, 5H), 2.98–2.81 (m, 2H), 2.70–2.55 (m, 2H); ^{13}C NMR (151 MHz, acetone-d_6) δ 200.7 (C-14), 150.9 (C-12), 146.6 (C-6), 135.7 (C-13), 114.2 (C-17), 90.5 (C-15), 80.2 (C-3), 68.8 (C-5), 55.0 (C-4), 50.1 (C-1), 38.6 (C-2), 37.0 (C-9), 35.3 (C-7), 29.5 (C-11), 29.2 (C-19), 26.0 (C-10), 22.5 (C-8), 16.7 (C-18), 15.0 (C-16), 13.0 (C-20), 5-*O*-phenylpropionyl: 172.9, 142.0, 129.3, 129.3, 129.3, 129.3, 127.0, 36.5, 31.6.

***(12E,2S,3S,4R,5R,9S,11R,15R)-5-Cinnamoyloxylathyra-6(17),12-dien-3,15-diol-14-one* (13).** Starting from cinnamic acid, the title compound was prepared following the same procedure used for the synthesis of **3** and was obtained as a colorless crystal (yield 69%). HRMS-ESI-TOF *m/z* calcd for $C_{29}H_{36}O_5Na$ $[M+Na]^+$ 487.2453, found 487.2455; mp: 108–110 °C; $[\alpha]_D^{20}$ +279° (*c* 2.4, acetone); ^{1}H NMR (600 MHz, acetone-d_6) δ 7.54 (br s,

1H, H-12), 6.23 (d, *J* = 10.4 Hz, 1H, H-5), 4.94 (s, 1H, H-17a), 4.75 (s, 1H, H-17b), 4.61 (s, 1H, OH-15), 4.29–4.23 (m, 1H, H-3), 3.94 (br s, 1H, OH-3), 3.26–3.12 (m, 1H, H-1α), 2.53 (dd, *J* = 10.5, 2.4 Hz, 1H, H-4), 2.34 (dd, *J* = 13.4, 5.8 Hz, 1H, H-7α), 2.14–2.03 (m, 2H, H-2, H-7β), 1.98–1.84 (m, 2H, H-8α, H-8β), 1.68 (s, 3H, H-20), 1.59 (dd, *J* = 13.8, 10.4 Hz, 1H, H-1β), 1.51 (dd, *J* = 11.7, 8.6 Hz, 1H, H-11), 1.32–1.21 (m, 1H, H-9), 1.20 (s, 3H, H-18), 1.18 (s, 3H, H-19), 1.07 (d, *J* = 6.8 Hz, 3H, H-16), 5-*O*-cinnamoyl: 7.70–7.63 (m, 3H), 7.47–7.39 (m, 3H), 6.53 (d, *J* = 16.0 Hz, 1H); ^{13}C NMR (151 MHz, acetone-d_6) δ 200.8 (C-14), 151.2 (C-12), 146.8 (C-6), 135.7 (C-13), 114.4 (C-17), 90.7 (C-15), 80.2 (C-3), 69.1 (C-5), 55.3 (C-4), 50.3 (C-1), 38.7 (C-2), 37.0 (C-9), 35.6 (C-7), 29.6 (C-11), 29.2 (C-19), 26.1 (C-10), 22.6 (C-8), 16.7 (C-18), 15.1 (C-16), 13.1 (C-20), 5-*O*-cinnamoyl: 167.1, 145.3, 135.8, 131.3, 130.0, 130.0, 129.2, 129.2, 119.7.

(12E,2S,3S,4R,5R,9S,11R,15R)-5-(1-Naphthylacetyloxy)lathyra-6(17),12-dien-3,15-diol-14-one **(14).** Starting from 1-naphthylacetic acid, the title compound was prepared following the same procedure used for the synthesis of **3** and was obtained as a white amorphous solid (yield 28%). HRMS-ESI-TOF *m/z* calcd for $C_{32}H_{38}O_5Na$ $[M+Na]^+$ 525.2601, found 525.2611; $[\alpha]_D^{20}$ +155° (*c* 0.1, acetone); ^{1}H NMR (600 MHz, acetone-d_6) δ 7.60–7.29 (m, 1H, H-12), 6.12 (d, *J* = 10.4 Hz, 1H, H-5), 4.86 (s, 1H, H-17a), 4.66 (s, 1H, H-17b), 4.60 (s, 1H, OH-15), 4.14–4.11 (m, 1H, H-3), 3.52 (s, 1H, OH-3), 3.18–3.10 (m, 1H, H-1α), 2.43 (dd, *J* = 10.4, 3.1 Hz, 1H, H-4), 2.24–2.16 (m, 1H, H-7α), 2.11–1.99 (m, 1H, H-2), 1.97–1.89 (m, 1H, H-7β), 1.80–1.70 (m, 2H, H-8α, H-8β), 1.64 (s, 3H,

H-20), 1.56 (dd, *J* = 13.9, 10.4 Hz, 1H, H-1*β*), 1.45 (dd, *J* = 11.7, 8.6 Hz, 1H, H-11), 1.22–1.15 (m, 1H, H-9), 1.13 (s, 3H, H-18), 1.11 (s, 3H, H-19), 1.05 (d, *J* = 6.8 Hz, 3H, H-16), 5-*O*-(1-naphthylacetyl): 8.05 (d, *J* = 7.6 Hz, 1H), 7.92 (dd, *J* = 7.0, 2.2 Hz, 1H), 7.84 (dd, *J* = 7.1, 2.0 Hz, 1H), 7.55–7.48 (m, 2H), 7.47–7.41 (m, 2H), 4.13 (s, 2H); ^{13}C NMR (151 MHz, acetone-d_6) δ 200.7 (C-14), 150.8 (C-12), 146.6 (C-6), 135.7 (C-13), 114.4 (C-17), 90.5 (C-15), 80.3 (C-3), 69.5 (C-5), 55.0 (C-4), 50.0 (C-1), 38.7 (C-2), 36.9 (C-9), 35.3 (C-7), 29.5 (C-11), 29.2 (C-19), 26.0 (C-10), 22.4 (C-8), 16.6 (C-18), 15.0 (C-16), 13.1 (C-20), 5-*O*-(1-naphthylacetyl): 171.8, 135.0, 133.4, 132.5, 129.6, 129.2, 128.8, 127.1, 126.7, 126.5, 125.3, 39.7.

(12E,2S,3S,4R,5R,9S,11R,15R)-3,5-Diacetoxylathyra-6(17),12-dien-15-ol-14-one **(15).** Starting from acetic anhydride in the solvent of EtOAc, the title compound was prepared following the same procedure used for the synthesis of **10** and was obtained as a white amorphous solid (yield 54%). HRMS-ESI-TOF *m/z* calcd for $C_{24}H_{34}O_6Na$ $[M+Na]^+$ 441.2253, found 441.2248; $[\alpha]_D^{20}$ +225° (*c* 1.0, acetone); ^{1}H NMR (600 MHz, acetone-d_6) δ 7.63 (br s, 1H, H-12), 6.03 (d, *J* = 9.2 Hz, 1H, H-5), 5.49 (t, *J* = 3.4 Hz, 1H, H-3), 4.93 (s, 1H, H-17a), 4.75 (s, 1H, H-17b), 4.36 (s, 1H, OH-15), 3.09 (br s, 1H, H-1*α*), 2.65 (dd, *J* = 10.2, 2.6 Hz, 1H, H-4), 2.31–2.19 (m, 1H, H-2), 2.23 (dd, *J* = 14.2, 7.2 Hz, 1H, H-7*α*), 2.09–1.97 (m, 1H, H-7*β*), 1.92–1.84 (m, 1H, H-8*α*), 1.78–1.57 (m, 1H, H-8*β*), 1.67 (br s, 3H, H-20), 1.61 (dd, *J* = 13.4, 11.5 Hz, 1H, H-1*β*), 1.49 (dd, *J* = 11.7, 8.5 Hz, 1H, H-11), 1.26–1.19 (m, 1H, H-9), 1.16 (s, 3H, H-19), 1.14 (s, 3H, H-18), 0.93 (d, *J* = 6.8 Hz, 3H,

H-16), 3-OAc: 1.99 (s, 3H), 5-OAc: 1.88 (s, 3H); ^{13}C NMR (151 MHz, acetone-d_6) δ 201.4 (C-14), 152.8 (C-12), 146.6 (C-6), 135.0 (C-13), 115.1 (C-17), 89.6 (C-15), 81.4 (C-3), 68.0 (C-5), 54.3 (C-4), 50.7 (C-1), 38.3 (C-2), 36.9 (C-9), 35.6 (C-7), 29.4 (C-11), 29.2 (C-19), 26.0 (C-10), 22.5 (C-8), 16.7 (C-18), 14.8 (C-16), 13.0 (C-20), 3-OAc: 171.2, 21.2, 5-OAc: 170.9, 21.4.

***(12E,2S,3S,4R,5R,9S,11R,15R)-3,5-Dipropionyloxylathyra-6(17),12-dien-15-ol-14-one* (16).** To a 0 °C solution of **2** (120 mg, 0.36 mmol) and propionic anhydride (185 μL, 1.44 mmol) in dry CH_2Cl_2 (4 mL) was added dropwise $BF_3{\cdot}Et_2O$ (181 μL, 1.47 mmol) under argon atmosphere. The resulting mixture was stirred for 1 h at 0 °C and diluted with CH_2Cl_2, followed by washing with $NaHCO_3$. The organic layer was dried over Na_2SO_4 and concentrated in vacuo. Further purification was performed on flash column chromatography (petroleum ether/EtOAc = 16:1) to afford **16** (79 mg, yield 49%, white amorphous solid). HRMS-ESI-TOF *m/z* calcd for $C_{26}H_{38}O_6Na$ $[M+Na]^+$ 469.2554, found 469.2561; $[\alpha]_D^{20}$ +285° (*c* 1.7, acetone); ^{1}H NMR (600 MHz, acetone-d_6) δ 7.67 (br s, 1H, H-12), 6.05 (br s, 1H, H-5), 5.51 (t, *J* = 3.5 Hz, 1H, H-3), 4.92 (s, 1H, H-17a), 4.75 (s, 1H, H-17b), 4.33 (s, 1H, OH-15), 3.09 (br s, 1H, H-1α), 2.67 (br d, *J* = 8.6 Hz, 1H, H-4), 2.40–2.24 (m, 1H, H-2), 2.24–2.15 (m, 1H, H-7α), 2.07–1.97 (m, 1H, H-7β), 1.92–1.86 (m, 1H, H-8α), 1.80–1.57 (m, 1H, H-8β), 1.68 (br s, 3H, H-20), 1.61 (dd, *J* = 13.6, 11.4 Hz, 1H, H-1β), 1.49 (dd, *J* = 11.8, 8.5 Hz, 1H, H-11), 1.26–1.18 (m, 1H, H-9), 1.16 (s, 3H, H-19), 1.15 (s, 3H, H-18), 0.92 (d, *J* = 6.8 Hz, 3H, H-16), 3-*O*-propionyl: 2.40–2.24

(m, 2H), 1.08 (t, J = 7.5 Hz, 3H), 5-*O*-propionyl: 2.24–2.15 (m, 2H), 1.01 (t, J = 7.5 Hz, 3H); ^{13}C NMR (151 MHz, acetone-d_6) δ 201.4 (C-14), 152.7 (C-12), 146.6 (C-6), 135.0 (C-13), 115.0 (C-17), 89.7 (C-15), 81.3 (C-3), 67.7 (C-5), 54.6 (C-4), 50.8 (C-1), 38.3 (C-2), 36.9 (C-9), 35.9 (C-7), 29.4 (C-11), 29.2 (C-19), 26.1 (C-10), 22.5 (C-8), 16.7 (C-18), 14.8 (C-16), 13.0 (C-20), 3-*O*-propionyl: 174.5, 28.1, 9.5, 5-*O*-propionyl: 174.2, 28.2, 9.3.

(12E,2S,3S,4R,5R,9S,11R,15R)-3,5-Dibutyryloxylathyra-6(17),12-dien-15-ol-14-one

(17). Starting from butyric anhydride, the title compound was prepared following the same procedure used for the synthesis of **16** and was obtained as a colorless crystal (yield 50%). HRMS-ESI-TOF *m/z* calcd for $C_{28}H_{42}O_6Na$ $[M+Na]^+$ 497.2865, found 497.6193; mp: 125–127 °C; $[\alpha]_D^{20}$ +213° (*c* 0.1, acetone); ^{1}H NMR (600 MHz, acetone-d_6) δ 7.68 (br s, 1H, H-12), 6.02 (d, J = 9.2 Hz, 1H, H-5), 5.51 (t, J = 3.4 Hz, 1H, H-3), 4.92 (s, 1H, H-17a), 4.75 (s, 1H, H-17b), 4.33 (s, 1H, OH-15), 3.09 (br s, 1H, H-1α), 2.67 (br d, J = 8.9 Hz, 1H, H-4), 2.37–2.20 (m, 2H, H-2, H-7α), 2.07–1.97 (m, 1H, H-7β), 1.92–1.86 (m, 1H, H-8α), 1.80−1.57 (m, 1H, H-8β), 1.68 (br s, 3H, H-20), 1.65–1.57 (m, 1H, H-1β), 1.51–1.46 (m, 1H, H-11), 1.26–1.20 (m, 1H, H-9), 1.17 (s, 3H, H-19), 1.15 (s, 3H, H-18), 0.92 (d, J = 6.7 Hz, 3H, H-16), 3-*O*-butyryl: 2.37–2.20 (m, 2H), 1.67–1.45 (m, 2H), 0.97–0.91 (m, 3H), 5-*O*-butyryl: 2.15 (td, J = 7.6, 1.6 Hz, 2H), 1.67–1.45 (m, 2H), 0.89 (t, J = 7.4 Hz, 3H); ^{13}C NMR (151 MHz, acetone-d_6) δ 201.4 (C-14), 153.0 (C-12), 146.6 (C-6), 135.0 (C-13), 115.0 (C-17), 89.7 (C-15), 81.3 (C-3), 67.7 (C-5), 54.5 (C-4), 50.9

(C-1), 38.4 (C-2), 36.9 (C-9), 36.2 (C-7), 29.4 (C-11), 29.2 (C-19), 26.1 (C-10), 22.7 (C-8), 16.7 (C-18), 14.9 (C-16), 13.1 (C-20), 3-*O*-butyryl: 173.7, 36.8, 19.0, 14.3, 5-*O*-butyryl: 173.3, 37.0, 19.0, 14.2.

***(12E,2S,3S,4R,5R,9S,11R,15R)-3,5-Dihexanoyloxylathyra-6(17),12-dien-15-ol-14-one* (18).** Starting from hexanoic anhydride, the title compound was prepared following the same procedure used for the synthesis of **16** and was obtained as a syrup (yield 40%). HRMS-ESI-TOF *m/z* calcd for $C_{32}H_{50}O_6Na$ $[M+Na]^+$ 553.3499, found 553.3500; $[\alpha]_D^{20}$ +304° (*c* 0.2, acetone); ^{1}H NMR (600 MHz, acetone-d_6) δ 7.69 (br s, 1H, H-12), 6.03 (br s, 1H, H-5), 5.51 (t, *J* = 3.4 Hz, 1H, H-3), 4.92 (s, 1H, H-17a), 4.75 (s, 1H, H-17b), 4.33 (s, 1H, OH-15), 3.09 (br s, 1H, H-1α), 2.66 (br d, *J* = 9.2 Hz, 1H, H-4), 2.40–2.20 (m, 2H, H-2, H-7α), 2.07–1.97 (m, 1H, H-7β), 1.92–1.86 (m, 1H, H-8α), 1.80–1.57 (m, 1H, H-8β), 1.68 (br s, 3H, H-20), 1.65–1.57 (m, 1H, H-1β), 1.51–1.46 (m, 1H, H-11), 1.26–1.20 (m, 1H, H-9), 1.17 (s, 3H, H-19), 1.15 (s, 3H, H-18), 0.92 (d, *J* = 6.9 Hz, 3H, M-16), 3-*O*-hexanoyl: 2.40–2.20 (m, 2H), 1.66–1.45 (m, 2H), 1.38–1.24 (m, 4H), 0.96–0.84 (m, 3H), 5-*O*-hexanoyl: 2.17 (br t, *J* = 7.5 Hz, 2H), 1.66–1.45 (m, 2H), 1.38–1.24 (m, 4H), 0.96–0.84 (m, 3H); ^{13}C NMR (151 MHz, acetone-d_6) δ 201.4 (C-14), 153.0 (C-12), 146.6 (C-6), 135.0 (C-13), 115.0 (C-17), 89.7 (C-15), 81.3 (C-3), 67.9 (C-5), 54.5 (C-4), 50.9 (C-1), 38.4 (C-2), 36.9 (C-9), 36.2 (C-7), 29.4 (C-11), 29.2 (C-19), 26.1 (C-10), 22.6 (C-8), 16.7 (C-18), 14.9 (C-16), 13.0 (C-20), 3-*O*-hexanoyl: 173.8, 34.8, 32.3, 25.3, 23.3, 14.4, 5-*O*-hexanoyl: 173.5, 34.9, 32.2, 25.3, 23.2, 14.4.

(12E,2S,3S,4R,5R,9S,11R,15R)-3,5-Dibenzoyloxylathyra-6(17),12-dien-15-ol-14-one **(19).** Starting from benzoyl chloride, the title compound was prepared following the same procedure used for the synthesis of **10** and was obtained as a colorless crystal (yield 54%). HRMS-ESI-TOF *m/z* calcd for $C_{34}H_{38}O_6Na$ $[M+Na]^+$ 565.2576, found 565.2561; mp: 159–161°C; $[\alpha]_D^{20}$ +320° (*c* 0.1, acetone); ^{1}H NMR (600 MHz, acetone-d_6) δ 7.65–7.23 (m, 1H, H-12), 6.41 (br s, 1H, H-5), 5.86 (t, *J* = 3.5 Hz, 1H, H-3), 5.00 (s, 2H, H-17a, H-17b), 4.90 (s, 1H, OH-15), 3.15–3.04 (m, 1H, H-1α), 3.00 (dd, *J* = 9.1, 2.5 Hz, 1H, H-4), 2.46 (br s, 1H, H-2), 2.32–2.22 (m, 1H, H-7α), 2.10–2.00 (m, 1H, H-7β), 1.93–1.86 (m, 1H, H-8α), 1.86–1.70 (m, 1H, H-8β), 1.83 (br s, 3H, H-20), 1.80 (dd, *J* = 13.5, 11.8 Hz, 1H, H-1β), 1.54 (dd, *J* = 11.6, 8.6 Hz, 1H, H-11), 1.32–1.23 (m, 1H, H-9), 1.21 (s, 3H, H-18), 1.18 (s, 3H, H-19), 0.93 (d, *J* = 6.8 Hz, 3H, H-16), 3-*O*-benzoyl: 7.89 (d, *J* = 7.3 Hz, 2H), 7.56 (t, *J* = 7.4 Hz, 1H), 7.40 (t, *J* = 7.7 Hz, 2H), 5-*O*-benzoyl: 7.71 (d, *J* = 7.2 Hz, 2H), 7.52 (t, *J* = 7.4 Hz, 1H), 7.33 (t, *J* = 7.6 Hz, 2H); ^{13}C NMR (151 MHz, acetone-d_6) δ 203.2 (C-14), 151.8 (C-12), 146.5 (C-6), 135.3 (C-13), 115.0 (C-17), 88.2 (C-15), 81.1 (C-3), 69.9 (C-5), 53.5 (C-4), 50.1 (C-1), 38.9 (C-2), 36.5 (C-9), 35.8 (C-7), 29.1 (C-19), 29.0 (C-11), 25.8 (C-10), 22.1 (C-8), 16.6 (C-18), 15.0 (C-16), 13.3 (C-20), 3-*O*-benzoyl: 166.4, 133.6, 131.5, 130.4, 130.4, 129.0, 129.0, 5-*O*-benzoyl: 166.1, 133.6, 131.5, 130.6, 130.6, 129.0, 129.0.

(12E,2S,3S,4R,5R,9S,11R,15R)-3,5-Diphenylacetyloxylathyra-6(17),12-dien-15-ol-14-one **(20).** Starting from phenylacetic acid, the title compound was prepared following the

same procedure used for the synthesis of **3** with reduplicated reaction time and equivalent weight (a colorless crystal, yield 33%). HRMS-ESI-TOF *m/z* calcd for $C_{36}H_{42}O_6Na$ $[M+Na]^+$ 593.2871, found 593.2874; mp: 104–106 °C; $[\alpha]_D^{20}$ +261° (*c* 0.1, acetone); ^1H NMR (600 MHz, acetone-d_6) δ 7.61 (br s, 1H, H-12), 6.00 (d, *J* = 10.5 Hz, 1H, H-5), 5.59 (t, *J* = 3.3 Hz, 1H, H-3), 4.92 (s, 1H, H-17a), 4.72 (s, 1H, H-17b), 3.08 (br s, 1H, H-1α), 2.68 (br d, *J* = 9.9 Hz, 1H, H-4), 2.26 (br s, 1H, H-2), 2.12 (dd, *J* = 13.9, 6.7 Hz, 1H, H-7α), 2.02–1.91 (m, 1H, H-7β), 1.89–1.80 (m, 1H, H-8α), 1.74–1.58 (m, 1H, H-8β), 1.64 (s, 3H, H-20), 1.47 (dd, *J* = 11.8, 8.4 Hz, 1H, H-11), 1.44–1.33 (m, 1H, H-1β), 1.24–1.18 (m, 1H, H-9), 1.17 (s, 3H, H-19), 1.17 (s, 3H, H-18), 0.84 (d, *J* = 6.8 Hz, 3H, H-16), 3-*O*-phenylacetyl: 7.39–7.20 (m, 5H), 3.72–3.58 (AB, 2H), 5-*O*-phenylacetyl: 7.39–7.20 (m, 5H), 3.58–3.46 (AB, 2H); ^{13}C NMR (151 MHz, acetone-d_6) δ 200.8 (C-14), 153.0 (C-12), 146.1 (C-6), 134.9 (C-13), 115.3 (C-17), 89.9 (C-15), 82.5 (C-3), 68.5 (C-5), 54.7 (C-4), 50.9 (C-1), 38.2 (C-2), 37.0 (C-9), 36.1 (C-7), 29.4 (C-11), 29.2 (C-19), 26.2 (C-10), 22.6 (C-8), 16.7 (C-18), 14.7 (C-16), 12.9 (C-20), 3-*O*-phenylacetyl: 171.8, 135.2, 130.6, 130.6, 129.3, 129.3, 127.8, 41.9, 5-*O*-phenylacetyl: 172.0, 135.7, 130.9, 130.9, 129.4, 129.4, 128.0, 41.8.

(12E,2S,3S,4R,5R,9S,11R,15R)-3,5-Diphenylpropionyloxylathyra-6(17),12-dien-15-ol-14-one **(21).** Starting from phenylpropionic acid, the title compound was prepared following the same procedure used for the synthesis of **3** with reduplicated rection time and equivalent weight (syrup, yield 40%). HRMS-ESI-TOF *m/z* calcd for $C_{38}H_{46}O_6Na$

$[M+Na]^+$ 621.3179, found 621.3187; $[\alpha]_D^{20}$ +688° (*c* 0.2, acetone); ^{1}H NMR (600 MHz, acetone-d_6) δ 7.70 (br s, 1H, H-12), 6.07 (br s, 1H, H-5), 5.55 (t, *J* = 3.4 Hz, 1H, H-3), 4.91 (s, 1H, H-17a), 4.75 (s, 1H, H-17b), 4.34 (s, 1H, OH-15), 3.08 (br s, 1H, H-1α), 2.77–2.59 (m, 1H, H-4), 2.26 (br s, 1H, H-2), 2.10–2.00 (m, 1H, H-7α), 1.98–1.87 (m, 1H, H-7β), 1.87–1.81 (m, 1H, H-8α), 1.78–1.52 (m, 1H, H-8β), 1.67 (s, 3H, H-20), 1.58 (dd, *J* = 13.0, 11.9 Hz, 1H, H-1β), 1.48 (dd, *J* = 11.7, 8.6 Hz, 1H, H-11), 1.25–1.18 (m, 1H, H-9), 1.16 (s, 3H, H-19), 1.14 (s, 3H, H-18), 0.83 (d, *J* = 6.8 Hz, 3H, H-16), 3-*O*-phenylpropionyl: 7.35–7.12 (m, 5H), 3.00–2.81 (m, 2H), 2.77–2.59 (m, 2H), 5-*O*-phenylpropionyl: 7.35–7.12 (m, 5H), 3.00–2.81 (m, 2H), 2.52 (t, *J* = 7.8 Hz, 2H); ^{13}C NMR (151 MHz, acetone-d_6) δ 201.4 (C-14), 153.0 (C-12), 146.4 (C-6), 135.0 (C-13), 115.2 (C-17), 89.7 (C-15), 81.8 (C-3), 68.3 (C-5), 54.6 (C-4), 50.8 (C-1), 38.3 (C-2), 36.9 (C-9), 36.0 (C-7), 29.4 (C-11), 29.2 (C-19), 26.1 (C-10), 22.7 (C-8), 16.7 (C-18), 14.7 (C-16), 13.0 (C-20), 3-*O*-phenylpropionyl: 173.3, 142.1, 129.4, 129.4, 129.4, 129.4, 127.1, 36.5, 31.5, 5-*O*-phenylpropionyl: 172.8, 142.0, 129.4, 129.4, 129.4, 129.4, 127.1, 36.8, 31.6.

***(12E,2S,3S,4R,5R,9S,11R,15R)-3,5-Di(1-naphthylacetyloxy)lathyra-6(17),12-dien-15-ol-14-one* (22).** Starting from 1-naphthylacetic acid, the title compound was prepared following the same procedure used for the synthesis of **3** with reduplicated reaction time and equivalent weight (syrup, yield 25%). HRMS-ESI-TOF *m/z* calcd for $C_{44}H_{46}O_6Na$ $[M+Na]^+$ 693.3184, found 693.3187; $[\alpha]_D^{20}$ +325° (*c* 0.3, acetone); ^{1}H NMR (600 MHz,

acetone-d_6) δ 7.63–7.40 (m, 1H, H-12), 5.88 (d, J = 10.8 Hz, 1H, H-5), 5.62 (t, J = 3.0 Hz, 1H, H-3), 4.90 (s, 1H, H-17a), 4.68 (s, 1H, H-17b), 3.00–2.81 (m, 1H, H-1α), 2.64 (br d, J = 9.4 Hz, 1H, H-4), 2.31–2.13 (br s, 2H, H-2), 2.14–2.00 (m, 1H, H-7α), 1.99–1.83 (m, 1H, H-7β), 1.82–1.73 (m, 1H, H-8α), 1.69–1.47 (m, 2H, H-8β, H-1β), 1.58 (br s, 3H, H-20), 1.43 (dd, J = 11.7, 8.5 Hz, 1H, H-11), 1.23–1.17 (m, 1H, H-9), 1.14 (s, 3H, H-19), 1.14 (s, 3H, H-18), 0.81 (d, J = 6.7 Hz, 3H, H-16), 3-*O*-(1-naphthylacetyl): 8.18 (d, J = 8.4 Hz, 1H), 7.94 (d, J = 8.0 Hz, 2H), 7.63–7.40 (m, 4H), 4.25–3.95 (AB, 2H), 5-*O*-(1-naphthylacetyl): 8.01 (d, J = 8.2 Hz, 1H), 7.87 (d, J = 8.1 Hz, 2H), 7.63–7.40 (m, 4H), 4.25–3.95 (AB, 2H); ^{13}C NMR (151 MHz, acetone-d_6) δ 200.5 (C-14), 153.4 (C-12), 145.9 (C-6), 134.8 (C-13), 115.8 (C-17), 89.8 (C-15), 83.0 (C-3), 69.0 (C-5), 54.8 (C-4), 51.0 (C-1), 38.3 (C-2), 37.0 (C-9), 36.3 (C-7), 29.5 (C-11), 29.2 (C-19), 26.2 (C-10), 22.8 (C-8), 16.9 (C-18), 14.7 (C-16), 12.8 (C-20), 3-*O*-(1-naphthylacetyl): 171.8, 135.0, 133.2, 132.2, 129.8, 129.5, 129.0, 127.5, 127.0, 126.6, 125.3, 39.8, 5-*O*-(1-naphthylacetyl): 172.3, 135.0, 133.5, 132.3, 129.6, 129.4, 128.9, 127.2, 126.8, 126.6, 125.1, 39.5.

(12E,2S,3S,4R,5R,9S,11R,15R)-5-Benzoyloxy-3-propionyloxylathyra-6(17),12-dien-15-ol-14-one **(23).** Starting from propionic anhydride and **10**, the title compound was prepared following the same procedure used for the synthesis of **16** and was obtained as a white amorphous solid (yield 55%). HRMS-ESI-TOF *m/z* calcd for $C_{30}H_{38}O_6Na$ $[M+Na]^+$ 517.2535, found 517.2561; $[\alpha]_D^{20}$ +255° (*c* 0.1, acetone); ^{1}H NMR (600 MHz, acetone-d_6) δ 7.86–7.36 (m, 1H, H-12), 6.37 (d, J = 7.3 Hz, 1H, H-5), 5.59 (t, J = 3.5 Hz, 1H, H-3),

5.00 (s, 1H, H-17a), 4.91 (s, 1H, H-17b), 4.49 (s, 1H, OH-15), 3.09 (br s, 1H, H-1α), 2.85 (br d, J = 9.5 Hz, 1H, H-4), 2.36–2.13 (m, 2H, H-2, H-7α), 2.11–2.03 (m, 1H, H-7β), 1.97–1.89 (m, 1H, H-8α), 1.87–1.77 (m, 1H, H-8β), 1.72 (s, 3H, H-20), 1.64 (dd, J = 13.3, 11.8 Hz, 1H, H-1β), 1.52 (dd, J = 11.7, 8.5 Hz, 1H, H-11), 1.28–1.22 (m, 1H, H-9), 1.19 (s, 3H, H-18), 1.18 (s, 3H, H-19), 0.89 (d, J = 6.8 Hz, 3H, H-16), 3-*O*-propionyl: 2.36–2.13 (m, 2H), 0.84 (t, J = 7.5 Hz, 3H), 5-*O*-benzoyl: 7.94 (d, J = 7.5 Hz, 2H), 7.59 (t, J = 7.4 Hz, 1H), 7.46 (t, J = 7.7 Hz, 2H); ^{13}C NMR (151 MHz, acetone-d_6) δ 201.4 (C-14), 152.0 (C-12), 146.4 (C-6), 135.0 (C-13), 115.2 (C-17), 89.3 (C-15), 80.9 (C-3), 69.1 (C-5), 54.0 (C-4), 50.4 (C-1), 38.5 (C-2), 36.7 (C-9), 35.5 (C-7), 29.3 (C-11), 29.1 (C-19), 25.9 (C-10), 22.4 (C-8), 16.6 (C-18), 14.9 (C-16), 13.0 (C-20), 3-*O*-propionyl: 173.8, 27.8, 9.2, 5-*O*-benzoyl: 166.5, 133.8, 131.4, 130.5, 130.5, 129.2, 129.2.

(12E,2S,3S,4R,5R,9S,11R,15R)-5-Phenylacetyloxy-3-propionyloxylathyra-6(17),12-die n-15-ol-14-one **(24).** Starting from propionic anhydride and **11**, the title compound was prepared following the same procedure used for the synthesis of **16** and was obtained as a colorless crystal (yield 25%). HRMS-ESI-TOF *m/z* calcd for $C_{31}H_{40}O_6Na$ $[M+Na]^+$ 531.2712, found 531.2717; mp: 117–119 °C; $[\alpha]_D^{20}$ +215° (*c* 0.1, acetone); ^{1}H NMR (600 MHz, acetone-d_6) δ 7.69 (br s, 1H, H-12), 6.04 (br s, 1H, H-5), 5.61 (t, J = 3.4 Hz, 1H, H-3), 4.91 (s, 1H, H-17a), 4.76 (s, 1H, H-17b), 4.36 (s, 1H, OH-15), 3.11 (br s, 1H, H-1α), 2.70 (br d, J = 9.1 Hz, 1H, H-4), 2.43–2.21 (m, 2H, H-2, H-7α), 2.14–2.07 (m, 1H, H-7β), 2.01–1.88 (m, 1H, H-8α), 1.86–1.78 (m, 1H, H-8β), 1.67 (br s, 3H, H-20), 1.64 (dd, J =

13.4, 11.6 Hz, 1H, H-1β), 1.48 (dd, J = 11.6, 8.6 Hz, 1H, H-11), 1.24–1.17 (m, 1H, H-9), 1.15 (s, 3H, H-19), 1.13 (s, 3H, H-18), 0.95 (d, J = 6.7 Hz, 3H, H-16), 3-*O*-propionyl: 2.43–2.21 (m, 2H), 1.06 (t, J = 7.5 Hz, 3H), 5-*O*-phenylacetyl: 7.35–7.13 (m, 5H), 3.52 (AB, 2H); ^{13}C NMR (151 MHz, acetone-d_6) δ 201.2 (C-14), 153.0 (C-12), 146.3 (C-6), 135.0 (C-13), 115.3 (C-17), 89.7 (C-15), 81.5 (C-3), 68.4 (C-5), 54.5 (C-4), 50.8 (C-1), 38.4 (C-2), 36.9 (C-9), 36.1 (C-7), 29.4 (C-11), 29.2 (C-19), 26.1 (C-10), 22.6 (C-8), 16.7 (C-18), 14.8 (C-16), 13.1 (C-20), 3-*O*-propionyl: 174.7, 28.2, 9.6, 5-*O*-phenylacetyl: 171.7, 41.8, 135.6, 130.6, 130.6, 129.2, 129.2, 127.8.

(12E,2S,3S,4R,5R,9S,11R,15R)-5-(1-Naphthylacetyloxy)-3-propionyloxylathyra-6(17),12-dien-15-ol-14-one **(25).** Starting from propionic anhydride and **14**, the title compound was prepared following the same procedure used for the synthesis of **16** and was obtained as a white amorphous solid (yield 37%). HRMS-ESI-TOF m/z calcd for $C_{35}H_{42}O_6Na$ $[M+Na]^+$ 581.2880, found 581.2874; $[\alpha]_D^{20}$ +143° (c 1.7, acetone); ^{1}H NMR (600 MHz, acetone-d_6) δ 7.67 (br s, 1H, H-12), 6.02 (br s, 1H, H-5), 5.68 (t, J = 3.4 Hz, 1H, H-3), 4.89 (s, 1H, H-17a), 4.75 (s, 1H, H-17b), 4.38 (s, 1H, OH-15), 3.13 (br s, 1H, H-1α), 2.71 (dd, J = 10.6, 3.0 Hz, 1H, H-4), 2.44–2.24 (m, 2H, H-2, H-7α), 2.14–2.06 (m, 1H, H-7β), 1.98–1.85 (m, 1H, H-8α), 1.77–1.68 (m, 1H, H-8β), 1.77–1.50 (m, 3H, H-20), 1.65 (dd, J = 13.5, 11.4 Hz, 1H, H-1β), 1.46 (dd, J = 11.7, 8.5 Hz, 1H, H-11), 1.18–1.14 (m, 1H, H-9), 1.13 (s, 3H, H-19), 1.09 (s, 3H, H-18), 0.98 (d, J = 6.7 Hz, 3H, H-16), 3-*O*-propionyl: 2.44–2.24 (m, 2H), 1.14–1.07 (m, 3H), 5-*O*-(1-naphthylacetyl): 7.96 (d, J

= 8.0 Hz, 1H), 7.93–7.89 (m, 1H), 7.83 (d, *J* = 8.0 Hz, 1H), 7.55–7.47 (m, 2H), 7.47–7.39 (m, 2H), 4.08–3.89 (AB, 2H); ^{13}C NMR (151 MHz, acetone-d_6) δ 200.7 (C-14), 153.1 (C-12), 146.3 (C-6), 135.0 (C-13), 115.3 (C-17), 89.8 (C-15), 81.6 (C-3), 68.7 (C-5), 54.7 (C-4), 50.8 (C-1), 38.4 (C-2), 36.8 (C-9), 36.3 (C-7), 29.3 (C-11), 29.1 (C-19), 26.0 (C-10), 22.5 (C-8), 16.6 (C-18), 14.8 (C-16), 13.0 (C-20), 3-*O*-propionyl: 174.9, 28.3, 9.7, 5-*O*-(1-naphthylacetyl): 171.8, 135.0, 133.5, 132.3, 129.6, 129.3, 128.8, 127.1, 126.7, 126.5, 125.1, 39.6.

(12E,2S,3S,4R,5R,9S,11R,15R)-3-Benzoyloxy-5-(1-naphthylacetyloxy)lathyra-6(17),12-dien-15-ol-14-one **(26).** Starting from benzoic anhydride and **14**, the title compound was prepared following the same procedure used for the synthesis of **16** and was obtained as a colorless crystal (yield 30%). HRMS-ESI-TOF *m/z* calcd for $C_{39}H_{42}O_6Na$ $[M+Na]^+$ 629.2876, found 629.2874; mp: 109–111 °C; $[\alpha]_D^{20}$ +156° (*c* 0.05, acetone); ^{1}H NMR (600 MHz, acetone-d_6) δ 7.89–7.55 (m, 1H, H-12), 6.07 (br s, 1H, H-5), 5.93 (t, *J* = 3.5 Hz, 1H, H-3), 4.87 (br s, 1H, H-17a), 4.87 (br s, 1H, OH-15), 4.85 (br s, 1H, H-17b), 3.08 (br s, 1H, H-1α), 2.85 (dd, *J* = 9.9, 3.5 Hz, 1H, H-4), 2.48 (br s, 1H, H-2), 2.12–1.99 (m, 1H, H-7α), 1.82 (dd, *J* = 13.6, 11.6 Hz, 1H, H-1β), 1.79 (br s, 3H, H-20), 1.89–1.73 (m, 1H, H-7β), 1.72–1.63 (m, 1H, H-8α), 1.55 (br s, 1H, H-8β), 1.48 (dd, *J* = 11.6, 8.7 Hz, 1H, H-11), 1.19–1.14 (m, 1H, H-9), 1.13 (s, 3H, H-19), 1.11 (s, 3H, H-18), 1.01 (d, *J* = 6.7 Hz, 3H, H-16), 3-*O*-benzoyl: 8.23 (d, *J* = 7.1 Hz, 2H), 7.62 (t, *J* = 7.5 Hz, 1H), 7.51 (t, *J* = 7.8 Hz, 2H), 5-*O*-(1-naphthylacetyl): 7.85 (d, *J* = 8.1 Hz, 1H), 7.79 (d, *J* = 8.2 Hz, 1H), 7.76

(d, *J* = 8.2 Hz, 1H), 7.45 (t, *J* = 7.4 Hz, 1H), 7.41 (t, *J* = 7.6 Hz, 1H), 7.34 (t, *J* = 7.6 Hz, 1H), 7.22 (d, *J* = 6.1 Hz, 1H), 4.00–3.76 (AB, 2H); ^{13}C NMR (151 MHz, acetone-d_6) δ 200.8 (C-14), 150.9 (C-12), 146.3 (C-6), 135.4 (C-13), 114.8 (C-17), 88.2 (C-15), 81.2 (C-3), 67.8 (C-5), 53.7 (C-4), 50.2 (C-1), 38.7 (C-2), 36.5 (C-9), 35.7 (C-7), 29.1 (C-19), 28.9 (C-11), 25.8 (C-10), 22.0 (C-8), 16.5 (C-18), 14.9 (C-16), 13.2 (C-20), 3-*O*-benzoyl: 167.2, 134.0, 132.2, 131.0, 131.0, 129.4, 129.4, 5-*O*-(1-naphthylacetyl): 171.0, 134.9, 133.3, 131.6, 129.4, 129.0, 128.6, 126.9, 126.5, 126.3, 125.1, 39.3.

(12E,2S,3S,4R,5R,9S,11R,15R)-5-Benzoyloxy-3-cinnamoyloxylathyra-6(17),12-dien-15-ol-14-one **(27).** Starting from cinnamoyl chloride and **10**, the title compound was prepared following the same procedure used for the synthesis of **16** and was obtained as a white amorphous solid (yield 76%). HRMS-ESI-TOF *m/z* calcd for $C_{36}H_{40}O_6Na$ $[M+Na]^+$ 591.2722, found 591.2717; $[\alpha]_D^{20}$ +231° (*c* 0.1, acetone); ^{1}H NMR (600 MHz, acetone-d_6) δ 7.74– 7.24 (m, 1H, H-12), 6.43 (br s, 1H, H-5), 5.70 (t, *J* = 3.3 Hz, 1H, H-3), 5.02 (s, 1H, H-17a), 4.95 (s, 1H, H-17b), 4.62 (s, 1H, OH-15), 3.17–3.05 (m, 1H, H-1α), 2.91 (dd, *J* = 9.3, 2.6 Hz, 1H, H-4), 2.37 (br s, 1H, H-2), 2.29 (br dd, *J* = 14.3, 6.9 Hz, 1H, H-7α), 2.12–2.00 (m, 1H, H-7β), 1.96–1.87 (m, 1H, H-8α), 1.87– 1.78 (m, 1H, H-8β), 1.76 (s, 3H, H-20), 1.69 (dd, *J* = 13.1, 12.1 Hz, 1H, H-1β), 1.53 (dd, *J* = 11.7, 8.5 Hz, 1H, H-11), 1.33–1.21 (m, 1H, H-9), 1.20 (s, 3H, H-18), 1.18 (s, 3H, H-19), 0.93 (d, *J* = 6.8 Hz, 3H, H-16), 3-*O*-cinnamoyl: 7.60–7.24 (m, 5H), 7.33 (d, *J* = 16.2 Hz, 1H), 6.47 (d, *J* = 16.0 Hz, 1H), 5-*O*-benzoyl: 7.85 (d, *J* = 7.5 Hz, 2H), 7.37 (t, *J* = 7.7 Hz, 2H), 7.60–7.49 (m, 1H);

^{13}C NMR (151 MHz, acetone-d_6) δ 201.8 (C-14), 151.5 (C-12), 146.7 (C-6), 135.1 (C-13), 115.2 (C-17), 89.0 (C-15), 81.3 (C-3), 69.1 (C-5), 53.9 (C-4), 50.4 (C-1), 38.9 (C-2), 36.7 (C-9), 35.3 (C-7), 29.4 (C-11), 29.2 (C-19), 26.0 (C-10), 22.5 (C-8), 16.7 (C-18), 15.0 (C-16), 13.1 (C-20), 3-*O*-cinnamoyl: 166.7, 145.0, 135.9, 131.1, 129.9, 129.9, 129.1, 129.1, 119.7, 5-*O*-benzoyl: 166.4, 133.7, 131.7, 130.6, 130.6, 129.1, 129.1.

***(2S,3S,4R,5R,11R,13R,15R)-3,5-Diacetoxy-11,15-epoxylathyra-6(17),9(10)-dien-14-one* (28).** To a solution of **15** (140 mg, 0.33 mmol) in dry toluene (4 mL), TMSOTf (one drop) were added at 0 °C under argon atmosphere. The reaction mixture was allowed to warm to room temperature and stirred for 2 h. The resulting mixture was diluted with CH_2Cl_2, and neutralised with saturated $NaHCO_3$. The organic extracts were washed with water and dried, and evaporated under reduced pressure. The residue was purified by flash column chromatography to afford **28** (98 mg, 71%, petroleum ether/EtOAc = 20:1) as a colorless crystal. HRMS-ESI-TOF *m/z* calcd for $C_{24}H_{34}O_6Na$ $[M+Na]^+$ 441.2223, found 441.2248; mp: 195–197 °C; $[\alpha]_D^{20}$ -0.18° (*c* 0.05, acetone); ^{1}H NMR (600 MHz, acetone-d_6) δ 5.38 (t, *J* = 4.2 Hz, 1H, H-3), 5.35 (d, *J* = 10.9 Hz, 1H, H-5), 5.04 (dd, *J* = 11.9, 3.4 Hz, 1H, H-11), 4.90 (s, 1H, H-17a), 4.81 (s, 1H, H-17b), 3.61 (dd, *J* = 10.9, 4.8 Hz, 1H, H-4), 2.94–2.85 (m, 1H, H-13), 2.66 (br t, *J* = 13.4 Hz, 1H, H-8α), 2.60 (br dd, *J* = 12.9, 6.7 Hz, 1H, H-7α), 2.45 (br dd, *J* = 14.0, 7.3 Hz, 1H, H-8β), 2.21 (br t, *J* = 13.0 Hz, 1H, H-7β), 2.10–2.06 (m, 1H, H-1α), 2.03–1.96 (m, 1H, H-2), 1.96–1.90 (m, 1H, H-12α), 1.89–1.81 (m, 1H, H-12β), 1.84–1.78 (m, 1H, H-1β), 1.73 (s, 3H, H-18), 1.69 (s,

3H, H-19), 1.00 (d, *J* = 6.4 Hz, 3H, H-20), 0.88 (d, *J* = 6.7 Hz, 3H, H-16), 3-OAc: 2.01 (s, 3H), 5-OAc: 1.86 (s, 3H); ^{13}C NMR (151 MHz, acetone-d_6) δ 211.9 (C-14), 153.2 (C-6), 136.4 (C-9), 126.5 (C-10), 114.8 (C-17), 88.5 (C-15), 77.9 (C-3), 73.0 (C-11), 70.1 (C-5), 57.0 (C-4), 47.0 (C-1), 39.0 (C-7), 38.9 (C-2), 38.1 (C-13), 37.1 (C-12), 27.2 (C-8), 21.1 (C-18), 20.9 (C-19), 14.4 (C-20), 13.5 (C-16), 3-OAc: 170.7, 20.8, 5-OAc: 170.7, 21.1.

***(2S,3S,4R,5R,9S,11R,12S,13R,15R)-3,5-Dibenzoyloxy-12,15-epoxylathyra-6(17)-en-14-one* (29).** Starting from **19**, the title compound was prepared following the same procedure used for the synthesis of **28** and was obtained as a colorless crystal (yield 72%). HRMS-ESI-TOF *m/z* calcd for $C_{34}H_{38}O_6Na$ $[M+Na]^+$ 565.2537, found 565.2561; mp: 184–186 °C; $[\alpha]_D^{20}$ +196° (*c* 0.1, acetone); ^{1}H NMR (600 MHz, acetone-d_6) δ 5.76 (d, *J* = 11.2 Hz, 1H, H-5), 5.71 (t, *J* = 3.4 Hz, 1H, H-3), 5.02 (s, 1H, H-17a), 4.93 (d, *J* = 9.1 Hz, 1H, H-12), 4.82 (s, 1H, H-17b), 3.48 (dd, *J* = 11.1, 3.9 Hz, 1H, H-4), 2.95–2.87 (m, 1H, H-13), 2.76–2.68 (m, 1H, H-2), 2.28–2.19 (m, 1H, H-7α), 2.19–2.11 (m, 3H, H-1α, H-7β, H-8α), 1.93–1.87 (m, 1H, H-8β), 1.79 (t, *J* = 13.0 Hz, 1H, H-1β), 1.35 (s, 3H, H-18), 1.22 (d, *J* = 7.8 Hz, 3H, H-20), 1.12 (s, 3H, H-19), 0.92 (d, *J* = 6.7 Hz, 3H, H-16), 0.75–0.71 (m, 1H, H-9), 0.71 (d, *J* = 9.1 Hz, 1H, H-11), 3-*O*-benzoyl: 8.03 (d, *J* = 7.2 Hz, 2H), 7.64 (t, *J* = 7.4 Hz, 1H), 7.50 (t, *J* = 7.7 Hz, 2H), 5-*O*-benzoyl: 7.92 (d, *J* = 7.2 Hz, 2H), 7.58 (t, *J* = 7.4 Hz, 1H), 7.45 (t, *J* = 7.7 Hz, 2H); ^{13}C NMR (151 MHz, acetone-d_6) δ 219.8 (C-14), 149.5 (C-6), 116.7 (C-17), 87.5 (C-15), 79.1 (C-3), 75.7 (C-12), 69.3 (C-5), 54.6 (C-4), 45.8 (C-1), 42.3 (C-13), 38.8 (C-2), 38.7 (C-7), 31.1 (C-11), 29.5 (C-19), 27.8 (C-9), 23.9

(C-8), 16.2 (C-10), 15.5 (C-18), 14.3 (C-16), 13.5 (C-20), 3-*O*-benzoyl: 166.0, 134.0, 131.6, 130.4, 130.4, 129.3, 129.3, 5-*O*-benzoyl: 166.4, 133.8, 131.9, 130.4, 130.4, 129.5, 129.5.

***(2S,3S,4R,5R,9S,11R,12S,13R,15R)-3,5-Diphenylacetyloxy-12,15-epoxylathyra-6(17)-en-14-one* (30).** Starting from **20**, the title compound was prepared following the same procedure used for the synthesis of **28** and was obtained as a syrup (yield 43%). HRMS-ESI-TOF *m/z* calcd for $C_{36}H_{42}O_6Na$ $[M+Na]^+$ 593.2896, found 593.2874; $[\alpha]_D^{20}$ +125° (*c* 0.4, acetone); ^{1}H NMR (600 MHz, acetone-d_6) δ 5.53 (d, J = 11.5 Hz, 1H, H-5), 5.42 (t, J = 3.8 Hz, 1H, H-3), 4.94 (s, 1H, H-17a), 4.75 (d, J = 9.3 Hz, 1H, H-12), 4.63 (s, 1H, H-17b), 3.15 (dd, J = 11.5, 4.3 Hz, 1H, H-4), 2.88–2.78 (m, 1H, H-13), 2.57 (dd, J = 13.0, 7.1 Hz, 1H, H-2), 2.13–1.96 (m, 3H, H-7α, H-7β, H-8α), 1.92 (dd, J = 12.8, 6.8 Hz, 1H, H-1α), 1.90–1.84 (m, 1H, H-8β), 1.40 (t, J = 13.1 Hz, 1H, H-1β), 1.20 (s, 3H, H-18), 1.14 (d, J = 7.7 Hz, 3H, H-20), 1.08 (s, 3H, H-19), 0.72 (d, J = 6.7 Hz, 3H, H-16), 0.69–0.64 (m, 1H, H-9), 0.63 (d, J = 9.1 Hz, 1H, H-11), 3-*O*-phenylacetyl: 7.32–7.22 (m, 5H), 3.63 (AB, 2H), 5-*O*-phenylacetyl: 7.32–7.22 (m, 5H), 3.54 (d, J = 4.4 Hz, 2H); ^{13}C NMR (151 MHz, acetone-d_6) δ 219.9 (C-14), 149.1 (C-6), 115.7 (C-17), 87.1 (C-15), 78.4 (C-3), 75.6 (C-12), 68.7 (C-5), 53.7 (C-4), 45.1 (C-1), 41.5 (C-13), 38.7 (C-2), 37.9 (C-7), 31.1 (C-11), 29.3 (C-19), 27.4 (C-9), 23.9 (C-8), 16.1 (C-10), 15.9 (C-18), 13.6 (C-16), 13.4 (C-20), 3-*O*-phenylacetyl: 171.5, 135.6, 130.6, 130.6, 129.2, 129.2, 127.8, 42.1, 5-*O*-phenylacetyl: 172.0, 135.6, 130.8, 130.8, 129.3, 129.3, 127.8, 42.1.

***(2S,3S,4R,5R,9S,11R,12S,13R,15R)-3,5-Diphenylpropionyloxy-12,15-epoxylathyra-6(17)-en-14-one* (31).** Starting from **21** the title compound was prepared following the same procedure used for the synthesis of **28** and was obtained as a white amorphous solid (yield 45%). HRMS-ESI-TOF *m/z* calcd for $C_{38}H_{46}O_6Na$ $[M+Na]^+$ 621.3197, found 621.3187; $[\alpha]_D^{20}$ +100° (*c* 0.1, acetone); ^{1}H NMR (600 MHz, acetone-d_6) δ 5.54 (d, J = 11.5 Hz, 1H, H-5), 5.41 (t, J = 3.7 Hz, 1H, H-3), 4.95 (s, 1H, H-17a), 4.80 (d, J = 9.2 Hz, 1H, H-12), 4.64 (s, 1H, H-17b), 3.15 (dd, J = 11.5, 4.3 Hz, 1H, H-4), 2.90–2.83 (m, 1H, H-13), 2.57 (dd, J = 12.2, 7.2 Hz, 1H, H-2), 2.13–1.96 (m, 4H, H-1α, H-7α, H-7β, H-8α), 1.91–1.84 (m, 1H, H-8β), 1.58 (t, J = 12.5 Hz, 1H, H-1β), 1.17 (s, 3H, H-18), 1.15 (d, J = 7.7 Hz, 3H, H-20), 1.07 (s, 3H, H-19), 0.77 (d, J = 6.4 Hz, 3H, H-16), 0.70–0.65 (m, 1H, H-9), 0.64 (d, J = 9.1 Hz, 1H, H-11), 3-*O*-phenylpropionyl: 7.32–7.14 (m, 5H), 3.03–2.92 (m, 2H), 2.69–2.65 (m, 2H), 5-*O*-phenylpropionyl: 7.32–7.14 (m, 5H) 2.89–2.83 (m, 2H), 2.53–2.49 (m, 2H); ^{13}C NMR (151 MHz, acetone-d_6) δ 219.9 (C-14), 149.1 (C-6), 115.9 (C-17), 87.3 (C-15), 78.2 (C-3), 75.5 (C-12), 68.2 (C-5), 53.8 (C-4), 45.4 (C-1), 42.2 (C-13), 38.7 (C-2), 37.9 (C-7), 31.0 (C-11), 29.3 (C-19), 27.6 (C-9), 23.8 (C-8), 16.1 (C-10), 15.7 (C-18), 13.8 (C-16), 13.4 (C-20), 3-*O*-phenylpropionyl: 172.6, 142.0, 129.4, 129.4, 129.4, 129.4, 127.1, 36.7, 31.6, 5-*O*-phenylpropionyl: 173.0, 142.0, 129.3, 129.3, 129.3, 129.3, 127.0, 36.7, 31.6.

***(2S,3S,4R,5R,9S,11R,12S,13S,15R)-3,5-Diacetoxy-12,15-epoxylathyra-6(17)-en-14-one* (32).** To a 0 °C solution of **15** (200 mg, 0.48 mmol) and DMAP (12 mg, 0.99 mmol) in

dry CH_2Cl_2 (4 mL) were added acetyl chloride (135 μL, 1.90 mmol) dropwise under argon atmosphere. The reaction was allowed to warm to room temperature and stirred for 8 h. After the reaction was completed, saturated $NaHCO_3$ were added and the reaction mixture was extracted with EtOAc. The combined organic phases were dried over $NaSO_4$, and concentrated. Further purification was performed by flash column chromatography (petroleum ether/EtOAc = 22:1) to give **32** as a syrup (131 mg, yield 65%). HRMS-ESI-TOF *m/z* calcd for $C_{24}H_{34}O_6Na$ $[M+Na]^+$ 441.2252, found 441.2248; $[\alpha]_D^{20}$ +113° (*c* 3.8, acetone); ^{1}H NMR (600 MHz, acetone-d_6) δ 5.45 (d, *J* = 11.5 Hz, 1H, H-5), 5.35 (t, *J* = 3.9 Hz, 1H, H-3), 4.98 (s, 1H, H-17a), 4.73 (s, 1H, H-17b), 4.16 (d, *J* = 9.9 Hz, 1H, H-12), 2.96 (dd, *J* = 11.5, 4.4 Hz, 1H, H-4), 2.62 (dd, *J* = 13.1, 7.2 Hz, 1H, H-2), 2.41 (dq, *J* = 9.9, 7.2 Hz, 1H, H-13), 2.18–2.07 (m, 3H, H-7α, H-7β, H-8α), 2.01–1.90 (m, 2H, H-1α, H-8β), 1.52 (t, *J* = 13.1 Hz, 1H, H-1β), 1.17 (s, 3H, H-18), 1.10 (d, *J* = 7.2 Hz, 3H, H-20), 1.08 (s, 3H, H-19), 0.89 (d, *J* = 6.8 Hz, 3H, H-16), 0.73 (d, *J* = 9.1 Hz, 1H, H-11), 0.67 (ddd, *J* = 11.6, 9.3, 4.0 Hz, 1H, H-9), 3-OAc: 1.99 (s, 3H), 5-OAc: 1.86 (s, 3H); ^{13}C NMR (151 MHz, acetone-d_6) δ 221.7 (C-14), 149.9 (C-6), 115.2 (C-17), 88.5 (C-15), 81.0 (C-12), 77.7 (C-3), 67.9 (C-5), 55.1 (C-4), 47.9 (C-13), 45.3 (C-1), 38.7 (C-2), 38.2 (C-7), 31.0 (C-11), 29.7 (C-9), 29.3 (C-19), 23.8 (C-8), 16.9 (C-10), 15.7 (C-18), 13.8 (C-16), 12.7 (C-20), 3-OAc: 170.9, 21.3, 5-OAc: 171.0, 21.1.

***(2S,3S,4R,5R,9S,11R,12S,13S,15R)-3,5-Dibutyryloxy-12,15-epoxylathyra-6(17)-en-14-one* (33).** Starting from **17**, the title compound was prepared following the same

procedure used for the synthesis of **32** and was obtained as a white amorphous solid (yield 74%). HRMS-ESI-TOF *m/z* calcd for $C_{28}H_{42}O_6Na$ $[M+Na]^+$497.2888, found 497.2874; $[\alpha]_D^{20}$ +118° (*c* 0.1, acetone); ^{1}H NMR (600 MHz, acetone-d_6) δ 5.46 (d, *J* = 11.4 Hz, 1H, H-5), 5.37 (t, *J* = 3.7 Hz, 1H, H-3), 4.97 (s, 1H, H-17a), 4.73 (s, 1H, H-17b), 4.17 (d, *J* = 9.9 Hz, 1H, H-12), 2.97 (dd, *J* = 11.3, 4.3 Hz, 1H, H-4), 2.66 (dd, *J* = 12.8, 7.6 Hz, 1H, H-2), 2.41 (dq, *J* = 9.6, 7.2 Hz, 1H, H-13), 2.18–2.06 (m, 3H, H-7α, H-7β, H-8α), 1.99 (dd, *J* = 12.8, 6.9 Hz, 1H, H-1α), 1.96–1.91 (m, 1H, H-8β), 1.57–1.49 (m, 1H, H-1β), 1.18 (s, 3H, H-18), 1.10 (d, *J* = 7.3 Hz, 3H, H-20), 1.08 (s, 3H, H-19), 0.89 (d, *J* = 6.7 Hz, 3H, H-16), 0.73 (d, *J* = 9.1 Hz, 1H, H-11), 0.71–0.63 (m, 1H, H-9), 3-*O*-butyryl: 2.30 (t, *J* = 7.4 Hz, 2H), 1.70–1.59 (m, 2H), 0.96 (t, *J* = 7.4 Hz, 3H), 5-*O*-butyryl: 2.13 (t, *J* = 7.4 Hz, 2H), 1.58–1.46 (m, 2H), 0.88 (t, *J* = 7.5 Hz, 3H); ^{13}C NMR (151 MHz, acetone-d_6) δ 221.7 (C-14), 150.2 (C-6), 115.2 (C-17), 88.6 (C-15), 81.0 (C-12), 77.6 (C-3), 67.8 (C-5), 55.3 (C-4), 47.9 (C-13), 45.5 (C-1), 38.8 (C-2), 38.4 (C-7), 30.9 (C-11), 29.7 (C-9), 29.4 (C-19), 23.8 (C-8), 16.9 (C-10), 15.7 (C-18), 14.3 (C-16), 12.8 (C-20), 3-*O*-butyryl: 173.1, 37.0, 19.1, 14.0, 5-*O*-butyryl: 173.4, 36.8, 19.1, 14.1.

(2S,3S,4R,5R,9S,11R,12S,13S,15R)-3,5-Dihexanoyloxy-12,15-epoxylathyra-6(17)-en-14-one **(34).** Starting from **18**, the title compound was prepared following the same procedure used for the synthesis of **32** and was obtained as a syrup (yield 56%). HRMS-ESI-TOF *m/z* calcd for $C_{32}H_{50}O_6Na$ $[M+Na]^+$ 553.3484, found 553.3500; $[\alpha]_D^{20}$ +180° (*c* 0.4, acetone); ^{1}H NMR (600 MHz, acetone-d_6) δ 5.45 (d, *J* = 11.3 Hz, 1H, H-5),

5.37 (t, *J* = 3.7 Hz, 1H, H-3), 4.97 (s, 1H, H-17a), 4.73 (s, 1H, H-17b), 4.16 (d, *J* = 9.9 Hz, 1H, H-12), 2.97 (dd, *J* = 11.4, 4.3 Hz, 1H, H-4), 2.67 (dd, *J* = 12.7, 7.5 Hz, 1H, H-2), 2.41 (dq, *J* = 9.7, 7.2 Hz, 1H, H-13), 2.18–2.06 (m, 3H, H-7*α*, H-7*β*, H-8*α*), 1.98 (dd, *J* = 12.8, 6.9 Hz, 1H, H-1*α*), 1.96–1.90 (m, 1H, H-8*β*), 1.55–1.49 (m, 1H, H-1*β*), 1.18 (s, 3H, H-18), 1.10 (d, *J* = 7.3 Hz, 3H, H-20), 1.09 (s, 3H, H-19), 0.89 (d, *J* = 6.8 Hz, 3H, H-16), 0.73 (d, *J* = 9.1 Hz, 1H, H-11), 0.70–0.62 (m, 1H, H-9), 3-*O*-hexanoyl: 2.31 (t, *J* = 7.6 Hz, 2H), 1.70–1.60 (m, 2H), 1.38–1.23 (m, 4H), 0.92 (t, *J* = 7.0 Hz, 3H), 5-*O*-hexanoyl: 2.15 (t, *J* = 7.5 Hz, 2H), 1.55–1.49 (m, 2H), 1.38–1.23 (m, 4H), 0.88 (t, *J* = 7.6 Hz, 3H); ^{13}C NMR (151 MHz, acetone-d_6) δ 221.7 (C-14), 150.3 (C-6), 115.2 (C-17), 88.6 (C-15), 81.0 (C-12), 77.6 (C-3), 67.9 (C-5), 55.4 (C-4), 47.9 (C-13), 45.6 (C-1), 38.9 (C-2), 38.5 (C-7), 31.0 (C-11), 29.8 (C-9), 29.4 (C-19), 23.9 (C-8), 17.0 (C-10), 15.9 (C-18), 14.1 (C-16), 12.9 (C-20), 3-*O*-hexanoyl: 173.3, 35.1, 32.2, 25.4, 23.3, 14.5, 5-*O*-hexanoyl: 173.6, 34.9, 32.4, 25.4, 23.4, 14.5.

***(2S,3S,4R,5R,9S,11R,12S,13S,15R)-3,5-Dibenzoyloxy-12,15-epoxylathyra-6(17)-en-14-one* (35).** Starting from **19**, the title compound was prepared following the same procedure used for the synthesis of **32** and was obtained as a colorless crystal (yield 61%). HRMS-ESI-TOF *m/z* calcd for $C_{34}H_{38}O_6Na$ $[M+Na]^+$ 565.2555, found 565.2561; mp: 194–196 °C; $[\alpha]_D^{20}$ +212° (*c* 0.1, acetone); ^{1}H NMR (600 MHz, acetone-d_6) δ 5.76 (d, *J* = 11.0 Hz, 1H, H-5), 5.70 (t, *J* = 3.5 Hz, 1H, H-3), 5.05 (s, 1H, H-17a), 4.92 (s, 1H, H-17b), 4.31 (d, *J* = 9.9 Hz, 1H, H-12), 3.34 (dd, *J* = 11.0, 3.9 Hz, 1H, H-4), 2.76 (dd, *J* = 13.3,

7.2 Hz, 1H, H-2), 2.51 (dq, *J* = 9.6, 7.2 Hz, 1H, H-13), 2.35–2.26 (m, 1H, H-7*α*), 2.24–2.17 (m, 2H, H-7*β*, H-8*α*), 2.14 (dd, *J* = 13.1, 7.1 Hz, 1H, H-1*α*), 2.01–1.92 (m, 1H, H-8*β*), 1.73 (t, *J* = 13.1 Hz, 1H, H-1*β*), 1.36 (s, 3H, H-18), 1.16 (d, *J* = 7.2 Hz, 3H, H-20), 1.13 (s, 3H, H-19), 0.93 (d, *J* = 6.7 Hz, 3H, H-16), 0.82 (d, *J* = 9.1 Hz, 1H, H-11), 0.73 (ddd, *J* = 11.4, 9.3, 4.1 Hz, 1H, H-9), 3-*O*-benzoyl: 8.03 (d, *J* = 7.3 Hz, 2H), 7.64 (t, *J* = 7.4 Hz, 1H), 7.50 (t, *J* = 7.8 Hz, 2H), 5-*O*-benzoyl: 7.92 (d, *J* = 7.2 Hz, 2H), 7.58 (t, *J* = 7.4 Hz, 1H), 7.45 (t, *J* = 7.7 Hz, 2H); ^{13}C NMR (151 MHz, acetone-d_6) *δ* 221.6 (C-14), 150.1 (C-6), 116.1 (C-17), 88.8 (C-15), 81.1 (C-12), 78.9 (C-3), 69.1 (C-5), 56.0 (C-4), 47.9 (C-13), 46.0 (C-1), 39.1 (C-2), 38.9 (C-7), 31.0 (C-11), 29.8 (C-9), 29.4 (C-19), 23.8 (C-8), 17.1 (C-10), 15.7 (C-18), 14.3 (C-16), 12.9 (C-20), 3-*O*-benzoyl: 166.0, 134.1, 131.8, 130.5, 130.5, 129.5, 129.5, 5-*O*-benzoyl: 166.4, 133.8, 131.6, 130.5, 130.5, 129.4, 129.4.

***(2S,3S,4R,5R,9S,11R,12S,13S,15R)-3,5-Diphenylacetyloxy-12,15-epoxylathyra-6(17)-en-14-one* (36).** Starting from **20**, the title compound was prepared following the same procedure used for the synthesis of **32** and was obtained as a colorless crystal (yield 59%). HRMS-ESI-TOF *m/z* calcd for $C_{36}H_{42}O_6Na$ $[M+Na]^+$ 593.2868, found 593.2874; mp: 124–125 °C; $[\alpha]_D^{20}$ +156° (*c* 0.1, acetone); ^{1}H NMR (600 MHz, acetone-d_6) *δ* 5.54 (d, *J* = 11.4 Hz, 1H, H-5), 5.41 (t, *J* = 3.8 Hz, 1H, H-3), 4.98 (s, 1H, H-17a), 4.74 (s, 1H, H-17b), 4.13 (d, *J* = 9.9 Hz, 1H, H-12), 3.00 (dd, *J* = 11.5, 4.3 Hz, 1H, H-4), 2.61 (dd, *J* = 13.0, 7.4 Hz, 1H, H-2), 2.40 (dq, *J* = 9.8, 7.2 Hz, 1H, H-13), 2.18–2.06 (m, 3H, H-7*α*, H-7*β*,

H-8α), 1.98–1.92 (m, 1H, H-8β), 1.88 (dd, J = 12.7, 6.8 Hz, 1H, H-1α), 1.33 (t, J = 13.1 Hz, 1H, H-1β), 1.21 (s, 3H, H-18), 1.09 (d, J = 7.1 Hz, 3H, H-20), 1.09 (s, 3H, H-19), 0.73 (d, J = 6.7 Hz, 3H, H-16), 0.72 (d, J = 8.9 Hz, 1H, H-11), 0.69–0.63 (m, 1H, H-9), 3-*O*-phenylacetyl: 7.31–7.23 (m, 5H), 3.63 (AB, 2H), 5-*O*-phenylacetyl: 7.31–7.23 (m, 5H), 3.54 (d, J = 4.4 Hz, 2H); ^{13}C NMR (151 MHz, acetone-d_6) δ 221.6 (C-14), 149.8 (C-6), 115.3 (C-17), 88.4 (C-15), 81.0 (C-12), 78.2 (C-3), 68.6 (C-5), 55.0 (C-4), 47.9 (C-13), 45.2 (C-1), 38.8 (C-2), 38.4 (C-7), 30.9 (C-11), 29.7 (C-9), 29.3 (C-19), 23.9 (C-8), 16.9 (C-10), 16.0 (C-18), 13.7 (C-16), 12.7 (C-20), 3-*O*-phenylacetyl: 171.6, 135.6, 130.7, 130.7, 129.3, 129.3, 127.8, 42.2, 5-*O*-phenylacetyl: 172.1, 135.6, 130.8, 130.8, 129.4, 129.4, 127.9, 41.6.

***(2S,3S,4R,5R,9S,11R,12S,13S,15R)-3,5-Diphenylpropionyloxy-12,15-epoxylathyra-6(17)-en-14-one* (37).** Starting from **21**, the title compound was prepared following the same procedure used for the synthesis of **32** and was obtained as a syrup (yield 63%). HRMS-ESI-TOF *m/z* calcd for $C_{37}H_{44}O_6Na$ $[M+Na]^+$ 621.3202, found 621.3187; $[\alpha]_D^{20}$ +119° (*c* 2.1, acetone); ^{1}H NMR (600 MHz, acetone-d_6) δ 5.55 (d, J = 11.4 Hz, 1H, H-5), 5.40 (t, J = 3.7 Hz, 1H, H-3), 4.98 (s, 1H, H-17a), 4.75 (s, 1H, H-17b), 4.17 (d, J = 9.9 Hz, 1H, H-12), 3.03–2.93 (m, 1H, H-4), 2.63–2.56 (m, 1H, H-2), 2.42 (dq, J = 9.8, 7.2 Hz, 1H, H-13), 2.18–2.08 (m, 3H, H-7α, H-7β, H-8α), 1.99–1.91 (m, 2H, H-1α, H-8β), 1.51 (t, J = 13.1 Hz, 1H, H-1β), 1.18 (s, 3H, H-18), 1.10 (d, J = 7.2 Hz, 3H, H-20), 1.08 (s, 3H, H-19), 0.78 (d, J = 6.7 Hz, 3H, H-16), 0.73 (d, J = 9.1 Hz, 1H, H-11), 0.70–0.64 (m, 1H,

H-9), 3-*O*-phenylpropionyl: 7.33–7.14 (m, 5H), 3.04–2.92 (m, 2H), 2.69–2.64 (m, 2H), 5-*O*-phenylpropionyl: 7.33–7.14 (m, 5H), 2.87 (t, J = 7.5 Hz, 2H), 2.54–2.47 (m, 2H); ^{13}C NMR (151 MHz, acetone-d_6) δ 221.6 (C-14), 149.7 (C-6), 115.4 (C-17), 88.7 (C-15), 81.0 (C-12), 77.9 (C-3), 68.1 (C-5), 55.2 (C-4), 47.9 (C-13), 45.4 (C-1), 38.7 (C-2), 38.4 (C-7), 31.0 (C-11), 29.7 (C-9), 29.3 (C-19), 23.8 (C-8), 16.9 (C-10), 15.8 (C-18), 13.8 (C-16), 12.8 (C-20), 3-*O*-phenylpropionyl: 172.6, 142.1, 129.5, 129.5, 129.4, 129.4, 127.1, 36.7, 31.6, 5-*O*-phenylpropionyl: 173.0, 142.0, 129.4, 129.4, 129.4, 129.4, 127.1, 36.7, 31.6.

(2S,3S,4R,5R,9S,11R,12S,13S,15R)-3,5-Dicinnamoyloxy-12,15-epoxylathyra-6(17)-en-14-one **(38).** Compound **2** (150 mg, 0.45 mmol) and cinnamoyl chloride (300 mg, 1.8 mmol) in dry CH_2Cl_2 (5 mL) was cooled to 0 °C, and $BF_3{\cdot}Et_2O$ (0.56 ml, 4.5 mmol) was added dropwise under argon atmosphere. After stirring at 0 °C for 30 min, the reaction mixture was diluted by EtOAc, followed by washing with $NaHCO_3$. The organic extracts were washed with water and dried, and the solvent was evaporated. The residue was purified by column chromatography to afford **38** (118 mg, 44%, petroleum ether/EtOAc, 24:1) as a white amorphous solid. HRMS-ESI-TOF *m/z* calcd for $C_{38}H_{42}O_6Na$ $[M+Na]^+$ 617.2873, found 617.2874; $[\alpha]_D^{20}$ +366° (*c* 0.1, acetone); ^{1}H NMR (600 MHz, acetone-d_6) δ 5.65 (d, J = 11.8 Hz, 1H, H-5), 5.55 (t, J = 3.8 Hz, 1H, H-3), 5.03 (s, 1H, H-17a), 4.84 (s, 1H, H-17b), 4.25 (d, J = 9.9 Hz, 1H, H-12), 3.16 (dd, J = 11.3, 4.3 Hz, 1H, H-4), 2.81–2.74 (m, 1H, H-2), 2.47 (dq, J = 9.9, 7.2 Hz, 1H, H-13), 2.30–2.12 (m, 3H, H-7α,

H-7β, H-8α), 2.10–1.95 (m, 2H, H-1α, H-8β), 1.66 (t, J = 13.1 Hz, 1H, H-1β), 1.30 (s, 3H, H-18), 1.14 (d, J = 7.2 Hz, 3H, H-20), 1.12 (s, 3H, H-19), 0.93 (d, J = 6.7 Hz, 3H, H-16), 0.78 (d, J = 9.1 Hz, 1H, H-11), 0.75–0.65 (m, 1H, H-9), 3-*O*-cinnamoyl: 7.66–7.40 (m, 6H), 6.49 (d, J = 16.1 Hz, 1H), 5-*O*-cinnamoyl: 7.66–7.40 (m, 6H), 6.42 (d, J = 16.0 Hz, 1H); ^{13}C NMR (151 MHz, acetone-d_6) δ 221.7 (C-14), 150.3 (C-6), 115.5 (C-17), 88.6 (C-15), 81.0 (C-12), 78.0 (C-3), 68.4 (C-5), 55.5 (C-4), 47.9 (C-13), 45.5 (C-1), 38.9 (C-2), 38.8 (C-7), 30.9 (C-11), 29.7 (C-9), 29.3 (C-19), 23.8 (C-8), 17.0 (C-10), 16.0 (C-18), 14.1 (C-16), 12.7 (C-20), 3-*O*-cinnamoyl: 166.2, 145.3, 135.7, 131.2, 129.9, 129.9, 129.2, 129.2, 119.4, 5-*O*-cinnamoyl: 166.6, 145.1, 135.7, 131.3, 130.0, 130.0, 129.2, 129.2, 119.4.

(2S,3S,4R,5R,9S,11R,12S,13S,15R)-3,5-Di(1-naphthylacetyloxy)-12,15-epoxylathyra-6(17)-en-14-one **(39).** Starting from **22**, the title compound was prepared following the same procedure used for the synthesis of **32** and was obtained as a syrup (yield 58%). HRMS-ESI-TOF *m/z* calcd for $C_{44}H_{46}O_6Na$ $[M+Na]^+$ 693.3206, found 693.3187; $[\alpha]_D^{20}$ +108° (*c* 0.1, acetone); ^{1}H NMR (600 MHz, acetone-d_6) δ 5.55 (d, J = 11.4 Hz, 1H, H-5), 5.46 (t, J = 3.8 Hz, 1H, H-3), 4.97 (s, 1H, H-17a), 4.72 (s, 1H, H-17b), 4.09–4.03 (m, 1H, H-12), 2.98 (dd, J = 11.5, 4.3 Hz, 1H, H-4), 2.60 (br dd, J = 13.4, 7.3 Hz, 1H, H-2), 2.36 (dq, J = 9.8, 7.2 Hz, 1H, H-13), 2.14–2.08 (m, 1H, H-7α), 2.04–1.99 (m, 2H, H-7β, H-8α), 1.94–1.85 (m, 1H, H-8β), 1.75 (br dd, J = 12.7, 6.8 Hz, 1H, H-1α), 1.17 (s, 3H, H-18), 1.10 (t, J = 11.1 Hz, 1H, H-1β), 1.07 (s, 3H, H-19), 1.05 (d, J = 7.2 Hz, 3H, H-20), 0.68

(d, J = 9.1 Hz, 1H, H-11), 0.66–0.60 (m, 1H, H-9), 0.55 (d, J = 6.7 Hz, 3H, H-16), 3-*O*-(1-naphthylacetyl): 8.09 (d, J = 8.2 Hz, 1H), 7.94–7.90 (m, 2H), 7.57–7.39 (m, 4H), 4.13–4.05 (m, AB, 2H), 5-*O*-(1-naphthylacetyl): 8.00 (d, J = 8.3 Hz, 1H), 7.87–7.81 (m, 2H), 7.57–7.39 (m, 4H), 4.07–3.96 (m, AB, 2H); ^{13}C NMR (151 MHz, acetone-d_6) δ 221.6 (C-14), 149.8 (C-6), 115.3 (C-17), 88.3 (C-15), 81.0 (C-12), 78.3 (C-3), 68.9 (C-5), 55.0 (C-4), 47.8 (C-13), 45.0 (C-1), 38.9 (C-2), 38.3 (C-7), 30.8 (C-11), 29.7 (C-9), 29.3 (C-19), 23.8 (C-8), 16.8 (C-10), 16.2 (C-18), 13.5 (C-16), 12.7 (C-20), 3-*O*-(1-naphthylacetyl): 171.7, 135.0, 133.3, 132.1, 129.6, 129.2, 128.8, 127.2, 126.7, 126.5, 125.2, 39.9, 5-*O*-(1-naphthylacetyl): 172.2, 133.5, 132.3, 129.7, 129.5, 128.8, 127.3, 126.7, 126.6, 125.3, 135.0, 39.5.

X-ray crystallography analysis. Single crystals of **2** were analyzed on an APEX DUO X-ray diffractometer (Bruker, Germany) equipped with Mo$K\alpha$ radiation (λ = 0.7107 Å). Crystals of **3**, **20**, **28**, **29** and **35** were analyzed on an Xcalibur E X-ray diffractometer (Oxford Diffraction, UK) equipped with Mo$K\alpha$ radiation (λ = 0.7107 Å). The diffraction data of **17** were collected on a Gemini S Ultra X-ray diffractometer (Oxford Diffraction, UK) equipped with Cu$K\alpha$ radiation (λ = 1.54184 Å). These structures were determined using direct methods and refined using full-matrix least-squares techniques. All non-hydrogen atoms were refined using anisotropic thermal parameters. Hydrogen atoms were located by geometrical calculations. The absolute configuration of **17** was confirmed by refinement of the Flack parameter. Crystallographic data have been

deposited at the Cambridge Crystallographic Data Centre, CCDC No. 711586 (**2**), 1055473 (**3**), 1055472 (**17**), 1055474 (**20**), 1055470 (**28**), 1055475 (**29**) and 1055471 (**35**). These data are available free of charge from The Cambridge Crystallographic Data Centre *via* www.ccdc.cam.ac.uk/data_request/cif.

Cell Culture. The human breast carcinoma cell line MCF-7 was obtained from ATCC (American Type Culture Collection), and an ADR-resistant cell line MCF-7/ADR was derived from the parent MCF-7 cell line *via* stepwise selection in increasing ADR concentrations as previously described.[46,28] Cells were cultured in RPMI-1640 medium (Invitrogen, USA) supplemented with 10% fetal bovine serum (Invitrogen), 100 IU/mL penicillin and 100 μg/mL streptomycin. All cells were maintained in a humidified atmosphere incubator containing 5% CO_2 at 37 °C.

Cytotoxicity Analysis. Cytotoxicity was determined using the SRB colorimetric assay. Taxol (Sigma, USA) was used as a positive control. Cells (1×10^4 cells/well) were seeded into 96-well plates filled with culture medium containing various concentrations of test samples for 48 h. The proliferated cells were fixed with 10% trichloroacetic acid and stained with 0.4% (w/v) SRB (Sigma) in 1% acetic acid for 15-30 min. The cells were washed with 10% acetic acid and extracted with 10 mM unbuffered Tris base. The optical density (OD) was measured at 490 nm using a SpectraMax Plus 384 microplate reader (Molecular Devices, USA).

MDR Reversal Activity. *Relative Enhancement of Drug Sensitivity.* The cytotoxicities of ADR, the samples (10 μM), and ADR in the presence of the samples were analyzed using the previously described SRB assay. Verapamil (Sigma) was used as a positive control, and PBS (phosphate-buffered saline) was used as a negative control. The relative enhancement intensity was calculated as follows: Relative enhancement of drug sensitivity = Inhibition rate (sample + ADR) - Inhibition rate (ADR) - Inhibition rate (sample). Inhibition rate = $(OD_{PBS} - OD_{sample/ADR/sample + ADR})/OD_{PBS} \times 100$.

EC_{50} and Reversal Fold. The cytotoxicities of ADR (11 concentration gradients) and ADR in the presence of 10 μM samples (11 concentration gradients) were analyzed using the previously described SRB assay. Verapamil was used as a positive control, and PBS was used as a negative control. EC_{50} (ADR) and EC_{50} (ADR + sample) were calculated according to the inhibition rate. All experiments were performed at least three times. The reversal fold is proportional to the intensity of inhibition of P-gp. Reversal fold = EC_{50} (ADR)/EC_{50} (sample + ADR).

Intracellular Accumulation of Rh123. MCF-7/ADR and MCF-7 cells were seeded into 24-well plates at a density of 2×10^6/well and were pretreated with samples (2, 10, and 20 μM) at 37°C for 1 h. The cells were incubated with 5 μM Rh123 (Sigma) in the dark at 37°C for an additional 1 h. The cells were washed twice with cold PBS, resuspended in PBS buffer and analyzed by flow cytometry (MoFlo™ XDP, Beckman Coulter, USA). Verapamil was evaluated at 20 μM as a positive control.

Quantum Chemical Calculations. Quantum chemical calculations were performed using the program Gaussian09.[47] The geometrical structures of **2**-**39** were constructed based on X-ray results of the representatives in Groups I-V. The initial structures were first optimized using the DFT method at B3LYP/6-31G* and then fully optimized using the DFT method at the B3LYP/6-311G** level of theory. For compounds **14**, **19** and **25**, the electrostatic potential was calculated at the B3LYP/6-311G** level of theory and mapped onto the electron density surface for each compound. The isovalue of 0.0004 electron/bohr^3 was selected for the definition of the density surface with a scale of -0.05266 (red) to 0.05266 hartree (blue).

Homology Modeling. The homology models of human P-gp were generated based on the murine P-gp (PDB ID: 3G5U; chain A; resolution: 3.8 Å). Models were generated using the program MODELLER 9v9 and the automodel protocol.[48] The sequence alignment proposed by Aller *et al*. was used to perform the calculation.[15] To correct the disruption in TM 12 of murine P-gp, a helix structure constraint was imposed between residues 977 and 1011 (murine P-gp numbering). In the modeling process, 500 different homology models were created and refined. The final model was selected according to the molpdf value, DOPE score and GA341 score and was further evaluated using the programs PROCHECK,[49] WHAT_CHECK,[50] and ERRAT.[51]

Docking Calculations. The AutoDock Vina program (version 1.1.2) was used for the docking studies.[52] The 3D structures of **14**, **19** and **25** were derived from quantum

chemical calculations. The search volume ($50 \times 50 \times 50$ Å^3) was initially the entire cavity of the homology model. The positions of three independent docking simulations were statistically counted, and the region with the highest occurrence rate was subsequently defined as a smaller grid box ($20 \times 20 \times 20$ Å^3). For each docking simulation, the results were evaluated in terms of total estimated binding energy.

Molecular Dynamics Simulations. MD simulations were performed on three docked complexes of **14**, **19** and **25**. To simulate the actual physiological environment of the P-gp receptor, each selected complex structure was embedded into a 100 × 100 Å membrane bilayer generated using VMD and then solvated with water molecules at each side of the lipid bilayer at least 15 Å away from the solvent boundary.[53] The position of the membrane for P-gp was determined according to data obtained from the OPM database.[54] Finally, the complex and the lipid bilayer were solvated in a periodic rectangular box of TIP3P water. While inserted, any POPC lipid molecules within 0.8 Å and water molecules within 3.8 Å of the receptor were removed. The geometry of **14**, **19** and **25** was optimized by performing *ab initio* electronic structure calculations at the HF/6-31G* level using the Gaussian09 program to determine the restrained electrostatic potential (RESP) fitted charges. The parameters for **14**, **19** and **25** were also generated using GAFF with the Antechamber module. Ten Cl^- counterions were added to neutralize the charge on the system. The modular lipid force field, Lipid11, was used for the dynamics of the POPC membrane bilayers.[55] The standard Amber ff12 force field was

used for the receptor. Prior to MD simulations, a series of energy minimizations were performed. The first 5000 steps of minimization were practiced on the hydrogen atoms to remove bad contacts, followed by 5000 steps for the water molecules. Subsequently, the environment (*i.e.*, POPC molecules, water molecules and counterions) were optimized using 50,000 steps of a combination of steepest descent and conjugate gradient methods. Additional optimization of the solvate system was implemented in four successive steps. First, 500-ps MD simulations were performed on the water molecules with the NVT ensemble at 300 K. The environment was then refined through 30,000 steps of energy minimization. Additional 500-ps MD simulations were performed on the POPC molecules with semi-isotropic pressure coupling at 300 K. Finally, the entire system was minimized for 10,000 cycles without any restraints. Using the Langevin temperature regulation scheme, the minimized complex structures were subjected to heating from 0 to 300 K under the NVT ensemble for 100 ps. Subsequently, 100 ps of density equilibration with the NVT ensemble, followed by constant pressure equilibration with semi-isotropic pressure coupling were performed. The production phase was run for 5 ns at 300 K and 1 atm semi-isotropic pressure scaling in the NPT ensemble. The particle mesh Ewald (PME) method was applied to treat long-range electrostatic interactions. A nonbonded cutoff of 10 Å was used to truncate long-range nonbonded van der Waals interactions. The lengths of covalent bonds involving hydrogen atoms were fixed using the SHAKE algorithm. For the entire simulation, the integration step size was taken as 2 fs. The CPPTRAJ module

was used to analyze the H-bonds. All molecular dynamics simulations were performed using the PMEMD module of Amber12.[56]

MM/PBSA Binding Energy Calculation and MM/GBSA Energy Decomposition. The relative binding energies of **14**, **19** and **25** to the P-gp receptor were evaluated using MM/PBSA in Amber12. The expectation value for the complex, protein, and ligand free energies were evaluated from 100 uncorrelated snapshots in the MD trajectories. Due to the expensive computational demand and no apparent improvement in most cases, the entropy (TΔS) was not considered here.[57,58] MM/GBSA energy decomposition was performed on the binding complexes of **14**, **19** and **25** to calculate the contribution of each residue to the total binding energy.

ASSOCIATED CONTENT

Supporting Information. Figures of crystal structures (**2**, **3** and **20**), physicochemical properties and the molecular electrophilicity indices of compounds **2**–**39**, and top 10 residues in the free energy decomposing of **14**, **19** and **25**. This material is available free of charge via the Internet at http://pubs.acs.org.

AUTHOR INFORMATION

Corresponding Author

* (W. J.) E-mail: jiaowei@cib.ac.cn; Tel: +86-28-82890819.

* (H. S.) E-mail: shaohw@cib.ac.cn, Tel: +86-28-82890818.

Notes

The authors declare no competing financial interest.

ACKNOWLEDGMENTS

This work was supported financially by National Natural Science Foundation of China (21002098), Western Light Talent Culture Project of CAS (Y1C1011) and Knowledge Innovation Frontier Project of CAS (08B104).

ABBREVIATIONS USED

ADR, adriamycin; ABC, ATP binding cassette; TM, transmembrane; Rh123, rhodamine-123; EDCI, *N*-(3-dimethylaminopropyl)-*N′*-ethylcarbodiimide hydrochloride; TMSOTf, trimethylsilyl trifluoromethanesulfonate; PAR, parental cell; VRP, verapamil; TPSA, topological polar surface area; MV, molecular volume; MR, molar refractivity; ASA, accessible solvent area; HBA, number of hydrogen bond acceptors; HBD, number of hydrogen bond donors; TMD, transmembrane domain; SRB, sulforhodamine B; POPC, palmitoyl-oleyl-phosphatidyl-choline

REFERENCES

1. Latest world cancer statistics. Global cancer burden rises to 14.1 million new cases in 2012: Marked increase in breast cancers must be addressed (Press Releases 2013 of International Agency for Research on Cancer, 12/12/2013); http://www.iarc.fr/en/media-centre/pr/2013/pdfs/pr223_E.pdf.
2. Li, Y.; Yuan, H.; Yang, K.; Xu, W.; Tang, W.; Li, X. The structure and functions of P-glycoprotein. *Curr. Med. Chem.* **2010**, *17*, 786–800.

3. Hortobagyi, G. N. Treatment of breast cancer. *New Engl. J. Med.* **1998**, *339*, 974–984.

4. Longley, D. B.; Johnston, P. G. Molecular mechanisms of drug resistance. *J. Pathol.* **2005**, *205*, 275–292.

5. Gottesman, M. M.; Fojo, T.; Bates, S. E. Multidrug resistance in cancer: role of ATP-dependent transporters. *Nat. Rev. Cancer* **2002**, *2*, 48–58.

6. Eckford, P. D. W.; Sharom, F. J. ABC efflux pump-based resistance to chemotherapy drugs. *Chem. Rev.* **2009**, *109,* 2989–3011.

7. Mechetner, E.; Kyshtoobayeva, A.; Zonis, S.; Kim, H.; Stroup, R.; Garcia, R.; Parker, R. J.; Fruehauf, J. P. Levels of multidrug resistance (MDR1) P-glycoprotein expression by human breast cancer correlate with *in vitro* resistance to taxol and doxorubicin. *Clin. Cancer Res.* **1998**, *4*, 389–98.

8. Thiebaut, F.; Tsuruo, T.; Hamada, H.; Gottesman, M. M.; Pastan, I.; Willingham, M. C. Cellular localization of the multidrug-resistance gene product P-glycoprotein in normal human tissues. *Proc. Natl. Acad. Sci. U.S.A.* **1987**, *84*, 7735–7738.

9. Edwards, J. E.; Alcorn, J.; Savolainen, J.; Anderson, B. D.; McNamara, P. J. Role of P-glycoprotein in distribution of nelfinavir across the blood-mammary tissue barrier and blood-brain barrier. *Antimicrob. Agents Chemother.* **2005**, *49*, 1626–1628.

10. Melaine, N.; Liénard, M. O.; Dorval, I.; Le Goascogne, C.; Lejeune, H.; Jégou, B. Multidrug resistance genes and p-glycoprotein in the testis of the rat, mouse, Guinea

pig, and human. *Biol. Reprod.* **2002**, *67*(6), 1699–1707.

11. Saito, T.; Zhang, Z. J.; Ohtsubo, T.; Noda, I.; Shibamori, Y.; Yamamoto, T.; Saito, H. Homozygous disruption of the mdrla P-glycoprotein gene affects blood-nerve barrier function in mice administered with neurotoxic drugs. *Acta Otolaryngol.* **2001**, *121*(6), 735–742.
12. Schinkel, A. H.; Jonker, J. W. Mammalian drug efflux transporters of the ATP binding cassette (ABC) family: an overview. *Adv. Drug Deliver. Rev.* **2003**, *55*, 3–29.
13. Higgins, C. F.; Gottesman, M. M. Is the multidrug transporter a flippase? *Trends Biochem. Sci.* **1992**, *17*(1), 18–21.
14. Aller, S. G.; Yu, J.; Ward, A.; Weng, Y.; Chittaboina, S.; Zhuo, R.; Harrell, P. M.; Trinh, Y. T.; Zhang, Q.; Urbatsch, I. L.; Chang, G. Structure of P-glycoprotein reveals a molecular basis for poly-specific drug binding. *Science* **2009**, *323*, 1718–1722.
15. Bruggemann, E. P.; Germann, U. A.; Gottesman, M. M.; Pastan, I. Two different regions of P-glycoprotein [corrected] are photoaffinity-labeled by azidopine. *J. Biol. Chem.* **1989**, *264*, 15483–15488.
16. Dey, S.; Ramachandra, M.; Pastan, I.; Gottesman, M. M. Evidence for two nonidentical drug-interaction sites in the human P-glycoprotein. *Proc. Natl. Acad. Sci. U.S.A.* **1997**, *94*, 10594– 10599.

17. Loo, T. W.; Clarke, D. M. Mutational analysis of ABC proteins. *Arch. Biochem. Biophys.* **2008**, *476*, 51–64.

18. Shi, Q. W.; Su, X. H.; Kiyota, H. Chemical and pharmacological research of the plants in genus *Euphorbia*. *Chem. Rev.* **2008**, *108,* 4295–4327.

19. Vasas, A.; Hohmann, J. *Euphorbia* diterpenes: isolation, structure, biological Activity, and synthesis (2008−2012). *Chem. Rev.* **2014**, *114*, 8579−8612.

20. Hohmann, J.; Molnár, J.; Rédei, D.; Evanics, F.; Forgo, P.; Kálmán, A. Discovery and biological evaluation of a new family of potent modulators of multidrug resistance: reversal of multidrug resistance of mouse lymphoma cells by new natural jatrophane diterpenoids isolated from *Euphorbia* species. *J. Med. Chem.* **2002**, *45*, 2425−2431.

21. Hohmann, J.; Rédei, D.; Forgo, P.; Molnár, J.; Dombi, G.; Zorig, T. Jatrophane diterpenoids from *Euphorbia mongolica* as modulators of the multidrug resistance of L5128 mouse lymphoma cells. *J. Nat. Prod.* **2003**, *66*, 976−979.

22. Corea, G.; Fattorusso, E.; Lanzotti, V.; Taglialatela-Scafati, O.; Appendino, G.; Ballero, M.; Simon, P. N.; Dumontet, C.; Di Pietro, A. Jatrophane diterpenes as P-glycoprotein inhibitors. First insights of structure–activity relationships and discovery of a new, powerful lead. *J. Med. Chem.* **2003**, *46*, 3395−3402.

23. Corea, G.; Fattorusso, E.; Taglialatela-Scafati, O.; Appendino, G.; Ballero, M.; Sirnon, P. N. L.; Dumontet, C.; Di Pietro, A. Modified jatrophane diterpenes as

modulators of multidrug resistance from *Euphorbia dendroides* L. *Bioorg. Med. Chem.* **2003**, *11*, 5221−5227.

24. Corea, G.; Fattorusso, E.; Lanzotti, V.; Motti, R.; Simon, P. N.; Dumontet, C.; Di Pietro, A. Jatrophane diterpenes as modulators of multidrug resistance. Advances of structure–activity relationships and discovery of the potent lead pepluanin A. *J. Med. Chem.* **2004**, *47*, 988−992.
25. Duarte, N.; Járdánházy, A.; Molnár, J.; Hilgeroth, A.; Ferreira, M. J. U. Synergistic interaction between P-glycoprotein modulators and epirubicine on resistant cancer cells. *Bioorg. Med. Chem.* **2008**, *16*, 9323–9330.
26. Duarte, N.; Varga, A.; Cherepnev, G.; Radics, R.; Molnar, J.; Ferreira, M. J. U. Apoptosis induction and modulation of P-glycoprotein mediated multidrug resistance by new macrocyclic lathyrane-type diterpenoids. *Bioorg. Med. Chem.* **2007**, *15*, 546−554.
27. Appendino, G.; Della Porta, C.; Conseil, G.; Sterner, O.; Mercalli, E.; Dumontet, C.; Di Pietro, A. A new P-glycoprotein inhibitor from the caper spurge (*Euphorbia lathyris*). *J. Nat. Prod.* **2003**, *66*, 140−142.
28. Reis, M.; Ferreira, R. J.; Santos, M. M. M.; dos Santos, D. J. V. A.; Molnár, J.; Ferreira, M. J. U. Enhancing macrocyclic diterpenes as multidrug-resistance reversers: structure–activity studies on Jolkinol D derivatives. *J. Med. Chem.* **2013**, *56*, 748−760.

29. Jiao, W.; Dong, W. W.; Li, Z. F.; Deng, M. C.; Lu, R. H. Lathyrane diterpenes from *Euphorbia lathyris* as modulators of multidrug resistance and their crystal structures. *Bioorg. Med. Chem.* **2009**, *17*, 4786–4792.

30. Bicchi, C.; Appendino, G.; Cordero, C.; Rubiolo, P.; Ortelli, D.; Veuthey, J. L. HPLC-UV and HPLC-positive-ESI-MS analysis of the diterpenoid fraction from Caper Spurge (*Euphorbia lathyris*) seed oil. *Phytochem. Anal.* **2001**, *12*, 255–262.

31. Tian, Y.; Xu, W.; Zhu, C.; Lin, S.; Li, Y.; Xiong, L.; Wang, S.; Wang, L.; Yang, Y.; Guo, Y.; Sun, H.; Wang, X.; Shi, J. Lathyrane diterpenoids from the roots of *Euphorbia micractina* and their biological activities. *J. Nat. Prod.* **2011**, *74*, 1221–1229.

32. Ferreira, A. M. V. D.; Carvalho, L. H. M.; Carvalho, M. J. M.; Sequeira, M. M.; Silva, A. M. S. Jatrophane and lathyrane diterpenoids from *Euphorbia hyberna* L. *Phytochemistry* **2002**, *61*, 373–377.

33. Appendino, G.; Tron, G. C.; Cravotto, G.; Palmisano, G.; Jakupovic, J. An expeditious procedure for the isolation of ingenol from the seeds of *Euphorbia lathyris*. *J. Nat. Prod.* **1999**, *62*, 76–79.

34. Hohmann, J.; Evanics, F.; Vasas, A.; Dombi, G.; Jerkovich, G.; Máthé, I. A novel lathyrane diterpenoid from the roots of *Euphorbia lathyris*. *J. Nat. Prod.* **1999**, *62*, 176–178.

35. Appendino, G.; Belloro, E.; Tron, G. C.; Jakupovic, J.; Ballero, M. Diterpenoids

from *Euphorbia pithyusa* subsp. *cupanii*. *J. Nat. Prod.* **1999**, *62*, 1399−1404.

36. Taylor, M. D.; Smith III, A. B.; Furst, G. T.; Gunasekara, S. P.; Bevelle, C. A.; Cordell, G. A.; Farnsworth, N. R.; Kupchan, S. M.; Uchida, H. Plant anticancer agents. 28. New antileukemic jatrophone derivatives from *Jatropha gossypiifolia*: structural and stereochemical assignment through nuclear magnetic resonance spectroscopy. *J. Am. Chem. Soc.* **1983**, *105*, 3177–3183.
37. Skehan, P.; Storeng, R.; Scudiero, D.; Monks, A.; McMahon, J.; Vistica, D.;Warren, J. T.; Bokesch, H.; Kenney, S.; Boyd, M. R. New colorimetric cytotoxicity assay for anticancer-drug screening. *JNCI-J. Natl. Cancer Inst.* **1990**, *82*, 1107–1112.
38. Parthasarathi, R.; Subramanian, V.; Royb D. R.; Chattaraj P. K. Electrophilicity index as a possible descriptor of biological activity. *Bioorg. Med. Chem.* **2004**, *12*, 5533–5543.
39. Chattaraj, P. K.; Giri, S.; Soma, D. Update 2 of: electrophilicity index, *Chem. Rev.* **2011**, *111*, PR43–PR75.
40. Li, D.; Chen, L.; Li, Y.; Tian, S.; Sun, H.; Hou, T. ADMET evaluation in drug discovery. 13. Development of *in silico* prediction models for P-glycoprotein substrates. *Mol. Pharmaceutics* **2014**, *11*, 716–726.
41. Ferreira, R. J.; dos Santos, D. J. V. A.; Ferreira, M. J. U.; Guedes, R. C. Toward a better pharmacophore description of P-glycoprotein modulators, based on macrocyclic diterpenes from *Euphorbia* species. *Chem. Inf. Model.* **2011**, *51*,

1315–1324.

42. Gleeson, M. P. Generation of a set of simple, interpretable ADMET rules of thumb. *J. Med. Chem.* **2008**, *51*, 817–834.

43. Altschul, S. F.; Madden, T. L.; Schäffer, A. A.; Zhang, J.; Zhang, Z.; Miller, W.; Lipman D. J. Gapped BLAST and PSI-BLAST: a new generation of protein database search programs. *Nucleic Acids Res.* **1997**, *25*, 3389–3402.

44. Loo, T. W.; Bartlett, M. C.; Clarke, D. M. Substrate-induced conformational changes in the transmembrane segments of human P-glycoprotein. Direct evidence for the substrate-induced fit mechanism for drug binding. *J. Biol. Chem.* **2003**, *278*, 13603–13606.

45. Martin, C.; Berridge, G.; Mistry, P.; Higgins, C.; Charlton, P.; Callaghan, R. The molecular interaction of the high affinity reversal agent XR9576 with P-glycoprotein. *Br. J. Pharmacol.* **1999**, *128*(2), 403–411.

46. Batist, G.; Tulpule, A.; Sinha, B. K.; Katki, A. G.; Myers, C. E.; Cowan, K. H. Overexpression of a novel anionic glutathione transferase in multidrug-resistant human breast cancer cells. *J. Biol. Chem*. **1986**, *261*, 5544–5549.

47. Frisch, M. J.; Trucks, G. W.; Schlegel, H. B.; Scuseria, G. E.; Robb, M. A.; Cheeseman, J. R.; Scalmani, G.; Barone, V.; Mennucci, B.; Petersson, G. A.; Nakatsuji, H.; Caricato, M.; Li, X.; Hratchian, H. P.; Izmaylov, A. F.; Bloino, J.; Zheng, G.; Sonnenberg, J. L.; Hada, M.; Ehara, M.; Toyota, K.; Fukuda, R.;

Hasegawa, J.; Ishida, M.; Nakajima, T.; Honda, Y.; Kitao, O.; Nakai, H.; Vreven, T.; Montgomery Jr, J. A.; Peralta, J. E.; Ogliaro, F.; Bearpark, M.; Heyd, J. J.; Brothers, E.; Kudin, K. N.; Staroverov, V. N.; Kobayashi, R.; Normand, J.; Raghavachari, K.; Rendell, A.; Burant, J. C.; Iyengar, S. S.; Tomasi, J.; Cossi, M.; Rega, N.; Millam, J. M.; Klene, M.; Knox, J. E.; Cross, J. B.; Bakken, V.; Adamo, C.; Jaramillo, J.; Gomperts, R.; Stratmann, R. E.; Yazyev, O.; Austin, A. J.; Cammi, R.; Pomelli, C.; Ochterski, J. W.; Martin, R. L.; Morokuma, K.; Zakrzewski, V. G.; Voth, G. A.; Salvador, P.; Dannenberg, J. J.; Dapprich, S.; Daniels, A. D.; Farkas, O.; Foresman, J. B.; Ortiz, J. V.; Cioslowski, J.; Fox, D. J. Gaussian 09, Revision A.02. Gaussian Inc, Wallingford, CT, **2009**.

48. Eswar, N.; Marti-Renom, M. A.; Webb, B.; Madhusudhan, M. S.; Eramian, D.; Shen, M.; Pieper, U.; Sali, A. Comparative protein structure modeling with MODELLER. *Current Protocols in Bioinformatics*; Wiley: New York, **2006**; Suppl. 15, pp 5.6.1–5.6.30.

49. Laskoswki, R. A.; MacArthur, M. W.; Moss, D. S.; Thorton, J. M. PROCHECK: a program to check the stereochemical quality of protein structures. *J. Appl. Crystallogr*. **1993**, *26*, 283–291.

50. Hooft, R. W.; Vriend, G.; Sander, C.; Abola, E. E. Errors in protein structures. *Nature* **1996**, *381*, 272.

51. Colovos, C.; Yeates, T. O. Verification of protein structures: patterns of nonbonded

atomic interactions. *Protein Sci.* **1993**, *2*, 1511−1519.

52. Trott, O.; Olson, A. J. AutoDock Vina: improving the speed and accuracy of docking with a new scoring function, efficient optimization and multithreading. *J. Comput. Chem.* **2010**, *31*, 455−461.

53. Humphrey, W.; Dalke, A.; Schulten, K. VMD: visual molecular dynamics. *J. Mol. Graphics* **1996**, *14*(1), 33.

54. Lomize, M. A.; Lomize, A. L.; Pogozheva, I. D.; Mosberg, H. I. OPM: orientations of proteins in membranes database. *Bioinformatics* **2006**, *22*, 623−625.

55. Skjevik, Å. A.; Madej, B. D.; Walker, R. C.; Teigen, K. LIPID11: a modular framework for lipid simulations using Amber. *J. Phys. Chem. B* **2012**, *116*, 11124−11136.

56. Case, D. A.; Darden, T. A.; Cheatham, T. E.; Simmerling, C. L.; Wang, J.; Duke, R. E.; Luo, R.; Walker, R. C.; Zhang, W.; Merz, K. M.; Roberts, B.; Hayik, S.; Roitberg, A.; Seabra, G.; Swails, J.; Goetz, A. W.; Kolossváry, I.; Wong, K. F.; Paesani, F.; Vanicek, J.; Wolf, R. M.; Liu, J.; Wu, X.; Brozell, S. R.; Steinbrecher, T.; Gohlke, H.; Cai, Q.; Ye, X.; Wang, J.; Hsieh, M. J.; Cui, G.; Roe, D. R.; Mathews, D. H.; Seetin, M. G.; Salomon-Ferrer, R.; Sagui, C.; Babin, V.; Luchko, T.; Gusarov, S.; Kovalenko, A.; Kollman, P. A. *AMBER 12*; University of California: San Francisco, CA, **2012**.

57. Hou, T.; Wang, J.; Li, Y.; Wang, W. Assessing the performance of the molecular

mechanics/Poisson Boltzmann surface area and molecular mechanics/generalized Born surface area methods. II. The accuracy of ranking poses generated from docking. *J. Comput. Chem.* **2011**, *32*, 866−877.

58. Genheden, S.; Kuhn, O.; Mikulskis, P.; Hoffmann, D.; Ryde, U. The normal-mode entropy in the MM/GBSA method: effect of system truncation, buffer region, and dielectric constant. *J. Chem. Inf. Model.* **2012**, *52*, 2079−2088.

Table of Contents Graphic